A new 3D temperature model for Ireland from joint geophysical-petrological inversion of seismic, surface heat flow and petrophysical data

Emma L. Chambers[1*], Javier Fullea[1,2], Duygu Kiyan[1,3], Sergei Lebedev[1,4], Christopher J. Bean[1,3], Pat Meere[3,5], J. Stephen Daly[6,3], Nicola Willmot Noller[6], Robert Raine[7], Sarah Blake[8], Brian M. O'Reilly[1,3]

1) School of Cosmic Physics, Dublin Institute for Advanced Studies, Dublin, Ireland
2) Department of Physics of the Earth and Astrophysics, Universidad Complutense de Madrid, Madrid, Spain
3) iCRAG, SFI Research Centre In Applied Geosciences, Dublin, Ireland
4) Department of Earth Sciences, University of Cambridge, Cambridge, UK
5) School of Biological, Earth & Environmental Sciences, University College Cork, Cork, Ireland
6) UCD School of Earth Sciences, University College Dublin, Dublin, Ireland
7) Geological Survey of Northern Ireland, British Geological Survey, Belfast, UK
8) Geological Survey Ireland, Dublin, Ireland

[*]Corresponding author. Email echambers@cp.dias.ie

Submitted to Geophysical Journal International (GJI)

A new 3D temperature model for Ireland from joint geophysical-petrological inversion of seismic, surface heat flow and petrophysical data

Emma L. Chambers[1*], Javier Fullea[1,2], Duygu Kiyan[1,3], Sergei Lebedev[1,4], Christopher J. Bean[1,3], Pat Meere[3,5], J. Stephen Daly[6,3], Nicola Willmot Noller[6], Robert Raine[7], Sarah Blake[8], Brian M. O'Reilly[1,3]

9) School of Cosmic Physics, Dublin Institute for Advanced Studies, Dublin, Ireland
10) Department of Physics of the Earth and Astrophysics, Universidad Complutense de Madrid, Madrid, Spain
11) iCRAG, SFI Research Centre In Applied Geosciences, Dublin, Ireland
12) Department of Earth Sciences, University of Cambridge, Cambridge, UK
13) School of Biological, Earth & Environmental Sciences, University College Cork, Cork, Ireland
14) UCD School of Earth Sciences, University College Dublin, Dublin, Ireland
15) Geological Survey of Northern Ireland, British Geological Survey, Belfast, UK
16) Geological Survey Ireland, Dublin, Ireland

[*]Corresponding author. Email echambers@cp.dias.ie

Keywords: Geothermal, temperature, joint inversion, surface waves, Ireland

Abstract

High-quality maps of subsurface temperature and the geothermal gradient are essential when assessing the geothermal potential of a region. However, determining geothermal potential is a challenge when direct measurements of *in-situ* temperature and thermal property information are sparse. In addition, indirect geophysical methods are sensitive to a range of parameters, not solely temperature. We determine the geothermal gradient across Ireland by inverting seismic, in addition to other geophysical and petrophysical input datasets, directly for temperature. The multi-parameter output models of the joint, geophysical-petrological, thermochemical inversion fit the input data and reveal the thermal structure within the crust and mantle, including the upper-crustal geothermal gradient (20 to 40 °C/km). Variations in the lithospheric thickness influence the temperature gradient, with thinner lithosphere resulting in elevated geotherms. In some locations, the observed geotherms are elevated further due to high radiogenic heat production in granitic rocks. In Northern Ireland a thin lithosphere coupled with a weakly conductive basalt layer overlying warm crust, results in elevated temperatures which call for further geothermal exploration. These are the first temperature maps for Ireland that include uncertainty estimates, providing ranges for the subsurface temperature values, and demonstrate that the maps are in good agreement with available direct borehole temperature measurements, which are observed to fall within the model uncertainty. Our new methodology provides workflows for determining the 3D geothermal potential in areas with limited direct temperature measurements. The final temperature model provides useful constraints for geothermal exploration and utilisation on the island of Ireland.

1 Introduction

A crucial parameter when assessing a geothermal resource is the crustal geothermal gradient which, traditionally, is derived directly from borehole measurements. However, in areas with few deep boreholes (>1000 m), there is uncertainty and limited knowledge of the subsurface properties; Ireland being one such location with <10 deep boreholes with temperature measurements (Fellgett & Monaghan, 2024). When assessing an area's geothermal potential and planning future projects for further exploration and development, a full 3D temperature model is required rather than disparate point measurements, because of rapid variations in subsurface geology making lateral interpolation highly uncertain. This 3D knowledge is required in order to develop renewable resources to meet Ireland's and

Northern Ireland's climate action plans, comply with the EU 2030 framework of climate and energy, and meet global climate targets (DECC, 2020, 2024; DfE, 2021; European Council, 2014).

To overcome limitations in available direct temperature measurements, it is possible to use indirect geophysical methods to model the geothermal gradient. A coherent characterization of the geothermal gradient near the surface implies a bottom to top heat flow approach where knowledge of the thermal thickness of the lithosphere (or lithosphere-asthenosphere boundary, LAB), the crust-mantle boundary (Moho), and crustal lithology (thermal conductivity and radiogenic heat production) are essential (Afonso et al., 2008; Cammarano et al., 2003; Chambers et al., 2023; Fullea et al., 2021; Kassa et al., 2022; Lebedev et al., 2024; Scheck-Wenderoth & Maystrenko, 2013).

Seismic data can provide information on the layer boundaries within the Earth and recent deployments in Ireland have produced new surface wave velocity models which are sensitive to these boundaries (Bonadio et al., 2021; Chambers et al., 2023) (Figure 1e). Recent thermal property datasets have also been collated to produce laterally continuous models for thermal conductivity in sediments and the upper crust (Figure 1c) (Chambers et al., 2023) and RHP (Figure 1d) (Willmot Noller & Daly, 2015). To produce a subsurface temperature map for all of Ireland, input datasets are required to cover each point in the model across the island. This includes point measurements which have been interpolated in previous studies (e.g. surface heat flow, Mather et al., (2018)).

The joint geophysical-petrological inversion workflow of Chambers et al., (2023) was used in this study to produce lithospheric temperature maps of Ireland with uncertainty and the resulting geothermal gradient. New maps of lithospheric and crustal thickness were also generated using this methodology. The new temperature maps suggest that subsurface temperatures at 2 km depth, are everywhere >60°C across the island of Ireland. The warmest temperatures are present in areas with large granitic bodies exposed at the surface with high radiogenic signatures, and in Northern Ireland beneath the basalts of the Antrim Lava Group, which is likely to act as an insulating blanket, and is coupled with the thinnest lithosphere on the island. The uncertainty analysis shows the variation in each point of the temperature maps providing ranges for the possible temperature values. The new temperature maps will be useful for future geothermal energy development in Ireland. This paper provides a proof of concept of the workflow and methodology that can be applied to other locations with sparse direct temperature measurements and limited subsurface datasets.

1.1 Deep Geothermal Studies in Europe

Previous studies have mapped lithospheric-scale thermal properties and the geothermal gradient using a variety of geophysical and geological datasets, and a range of modelling techniques across a variety of environments and scales (e.g. Anikiev et al., 2019; Békési et al., 2018; Cloetingh et al., 2010; Frey et al., 2022; Freymark et al., 2017; Lenkey et al., 2017; Majorowicz et al., 2019; Poulsen et al., 2015; Scheck-Wenderoth et al., 2014; Torne et al., 2023). The number of deep geothermal projects (exploiting geothermal resources from depths >400 m) is rising. Within Europe multiple projects are investigating the deep geothermal potential in areas such as Denmark (Poulsen et al., 2015, 2017), the Netherlands (Békési et al., 2020), the Upper Rhine Graben (Frey et al., 2022; Ledésert & Hébert, 2020), throughout the entirety of Turkey for both heat and electricity (Mertoglu et al., 2019; Serpen & DiPippo, 2022), and the Alpine–Pannonian transition zone (Lenkey et al., 2017). These are all well established geothermal areas, but not traditionally considered as typical geothermal settings when compared to volcanic regions. In Iceland, where geothermal is also an established high-enthalpy resource, improvements in technology now allow geothermal energy to be extracted from low enthalpy regions and from greater depths (Axelsson et al., 2010; Fridleifsson & Elders, 2005). Due to heat sources coming from both the crust and mantle, many studies model the subsurface temperature of a geothermal system at a lithospheric scale using thermal property data combined with geophysical datasets and various

modelling techniques (Békési et al., 2018; Cloetingh et al., 2010; Limberger, van Wees, et al., 2018; Poulsen et al., 2017; Scheck-Wenderoth et al., 2014; Scheck-Wenderoth & Maystrenko, 2013). These models then provide information on suitable areas for further shallow investigations before deep drilling. Modelling the subsurface geotherms allows de-risking the elevated cost of drilling thus providing a more targeted approach for future investigations.

Closer to Ireland, deep geothermal has been used sporadically for decades in Great Britain (GB) (e.g. Abesser et al., 2020; Busby, 2014; Downing & Gray, 1985, 1986; Younger et al., 2012). Since 1979 Southampton has been producing geothermal heat, and combined heat and power, for the civic centre, surrounding businesses and >1000 residential properties (geothermal gradient of 38.5 °C/km, Downing & Gray, 1986; Raine & Reay, 2019). More recently, the Eden Geothermal and United Downs projects aim to extract geothermal heat from granitic rocks (Abesser et al., 2020; Gan et al., 2021; Reinecker et al., 2021) with the United Downs project successfully drilling 2 deep geothermal wells to 2.5 and 5 km depth (Reinecker et al., 2021), measuring temperatures of ~180 °C at 5 km depth (Abesser et al., 2020). The islands of Ireland and Great Britain have some similarities in their geological histories, including the emplacement of granite sequences and the continuation of lithological units from Ireland across to Scotland (e.g. Daly, 2009; Dewey & Strachan, 2002; Woodcock & Strachan, 2009). The two location also have comparable surface heat flow values (Mather & Fullea, 2019), making it likely that geothermal resources can also be utilised in Ireland.

1.2 Geothermal studies in Ireland

Multiple geothermal studies have been conducted in Ireland including an initial study in 2004 to produce subsurface temperature maps of Ireland's shallow subsurface (Goodman et al., 2004; Jones et al., 2007). The IRETHERM project (2011-2016) sought to quantify Ireland's geothermal energy potential through integrated lithospheric modelling of geophysical and petrological data (Farrell et al., 2015; Fullea et al., 2014; Jones et al., 2014; Raine & Reay, 2019) and modelling magnetotelluric (MT) data with the aim of investigating sedimentary basins with elevated fluid temperatures (Campanyà et al., 2015; Delhaye et al., 2017, 2019; Vozar et al., 2020), identifying fluid circulation pathways of warm springs (Blake et al., 2021; Blake, Henry, Muller, et al., 2016; Blake, Henry, Murray, et al., 2016) and characterising Irish granites (Farrell et al., 2015; Fritschle et al., 2015).

More recently the GEO-URBAN project focussed on Vallès (Spain) and the Dublin Basin (Ireland) combining passive seismic, MT and structural geology information to characterise low enthalpy geothermal potential in an urban environment with major fault structures acting as potential fluid pathways (Maggio et al., 2021, 2022; Vozar et al., 2020). In addition, recent drilling by Geological Survey Ireland (GSI) at the Technical University, Dublin (TUD) Grangegorman campus in 2023, revealed a subsurface temperature of 38.5 °C at 1 km depth (Blake, *Pers. Comm*).

Through other projects, subsurface temperature maps have been produced for Ireland from 0 to 5 km depth by CSA for the Sustainable Energy Authority of Ireland (Goodman et al., 2004) and the G.O.THERM.3D project (Mather et al., 2018; Mather & Fullea, 2019) from 2 to 5 km depth. The study of Goodman et al., (2004), used temperature data from 117 boreholes from 10 m up to 2500 m deep and interpolated the geothermal gradient using a natural neighbour interpolation to a 1000 m deep model. From 1000 to 5000m the geothermal gradient was linearly extrapolated due to limited measurements. Near-surface temperature effects (e.g. paleoclimate effects), variations in rock thermal properties and deep lithospheric contributions were not considered. The G.O.THERM.3D project modelled crustal layer thickness using receiver functions (Licciardi et al., 2014), controlled source seismic data (Hauser et al., 2008; Landes et al., 2005), crustal magnetic anomalies (Baykiev et al., 2018; Mather & Fullea, 2019), lithospheric thickness (Fullea et al., 2014) and surface heat flow from historic wells in Ireland (Brock, 1989; Brock & Barton, 1987) and applied paleoclimate corrections (Mather et al., 2018; Mather

& Fullea, 2019), producing temperature maps from 1 to 5 km depth. The datasets and models along with fixed crustal thermal property data (van den Berg et al., 2005), were inverted for crustal temperature with models showing geothermal gradients >20 °C/km everywhere matching well to global models of geothermal gradient (Limberger, Boxem, et al., 2018). These models predicted exceptionally high temperatures in Northern Ireland beneath basaltic intrusions, which were as high as magmatic high enthalpy geothermal settings. While Goodman et al., (2004) and Mather et al., (2018) provided valuable information on the subsurface temperatures and geothermal gradient in Ireland, the models are limited by their use of fixed parameters for lithospheric thickness and for the crustal thermal parameters that directly control the subsurface temperatures. Furthermore, the models have no uncertainty associated with them. Estimating uncertainty in the models is crucial to initiate geothermal extraction as it allows the determination of risk associated with drilling and exploitation

Ongoing projects in Ireland include the De-risking Ireland's Geothermal potential project (DIG) which is an interdisciplinary project from the full island scale to the local scale of the Mallow warm spring region (Kiyan et al., 2022; O'Reilly et al., 2021). Geophysical surveys including passive seismic and magnetotellurics, in addition to geological field campaigns and hydrochemistry, are being combined to improve our understanding of a known geothermal system (Chambers et al., 2023; Kiyan et al., 2022; O'Reilly et al., 2021). Additionally, GSI's National Geothermal Database is currently being developed and Project InnerSpace (projectinnerspace.org) has a focus on developing geothermal energy usage in Northern Ireland and globally. As part of the efforts to improve the previous subsurface maps of Ireland within the DIG project, we have applied indirect geophysical methods with variable thermal property data to model the geothermal gradient, and benchmarked the models against direct temperature measurements. We provide the first uncertainty maps for subsurface temperature in Ireland, and new Radiogenic heat production, LAB and Moho depth maps.

2 Geological Background

The geological evolution of Ireland's crust began in the Precambrian era (Daly, 2009) and culminated in the amalgamation of continental and island arc components during the early Palaeozoic (Graham et al., 2009; Hauser et al., 2008; Mitchell, 2004; O'Reilly et al., 2006; Woodcock & Strachan, 2009). The convergence of the Laurentian and Avalonian continental domains represents the final major event in the formation of Ireland's continental lithosphere forming the supercontinent Laurasia. During the closure of the Iapetus Ocean, the distribution of radiogenic heat-producing elements in the Irish crust was likely influenced by the process of continental suturing (Herrington et al., 2018; van den Berg et al., 2005; Willmot Noller & Daly, 2015). However, detailed knowledge regarding radiogenic heat production values and their depth distribution across different tectonic terranes remains limited (Lee et al., 1987; Mather et al., 2018), although new HPR values for lower crustal xenoliths have recently been acquired (Daly, personal communication).

Transitioning from late orogenic pull-apart basins to mid-late Devonian, extensional sedimentary basins marked a significant change in plate-tectonic configuration (Hauser et al., 2008). These basins, particularly the Munster Basin, are a particular focus of recent geothermal projects due to the presence of warm springs (Blake, Henry, Muller, et al., 2016; O'Reilly et al., 2021). Central Ireland is predominantly covered by tropical shallow to deep-water carbonates, deposited in basins in response to marine transgressions. The distribution of carbonate facies is complex and controlled by extensional tectonics, which reactivated major faults in the accreted Caledonian basement. They also influence thermal conductivity values through variations in the mud and silica content (Clauser & Huenges, 1995; English et al., 2022; Förster et al., 2021; Long et al., 2018; Somerton, 1992).

The Variscan orogeny was most intense in the Munster Basin, where strong tectonic fabrics developed, inverting normal faults into steep-dipping reverse faults with widespread folding, faulting and metamorphism in southern and eastern Ireland (Meere et al., 2013; Shannon, 2018). Following the Variscan orogeny a period of rifting ensued in the Permian and again in the Early Triassic and was responsible for a number of grabens that developed across Ireland, forming the Kingscourt Inlier in Co. Cavan, and a number of basins across the NE of Ireland (Newtownards Trough, Larne Basin, Lough Neagh Basin, Rathlin Basin, Foyle Basin) (Johnston, 2004; Naylor, 1992). In northeast Ireland, Mesozoic to Cenozoic sedimentary rocks are present in extensional basins, offering geothermal reservoir potential in porous sands within basins like the Larne Basin (Raine & Reay, 2019). The British and Irish Palaeocene Igneous Province was also deposited in northeast Ireland with Palaeocene flood basalt formations (Antrim Lava Group), covering older sedimentary sequences and creating striking landscapes like the Giant's Causeway in Northern Ireland (Cooper, 2004; Cooper et al., 2008, 2012). Uplift of the lavas and erosion during the Eocene, Alpine compression and development of localised pull-apart basins during the Oligo-Miocene deposited clays and lignite in NE Ireland (Quinn, 2006). Significant intrusive activity also occurred at this time emplacing granite complexes such as the Mourne granites.

During the Pleistocene, Ireland experienced several glaciations, with a significant thickness of ice that cooled the crust (Mather et al., 2018) and removed much sedimentary cover and sculpted its landscape, leaving behind features like drumlins, eskers, and U-shaped valleys.

3 Methods and Data

A joint geophysical-petrological inversion scheme is used to compute seismic velocities and density in the mantle as a function of temperature and bulk composition within a thermodynamic framework (Afonso et al., 2008; Chambers et al., 2023; Fullea et al., 2009, 2021; Lebedev et al., 2024). Surface-wave seismic data alongside elevation are primarily used to constrain the upper mantle thermochemical structure and lithospheric boundaries, while thermal property data, surface heat flow and Moho depth constrain the crustal thermal structure.

Within the joint geophysical- petrological scheme the lithospheric geotherm is computed by solving the heat conduction equation in the lithosphere for a given distribution of thermal conductivity and radiogenic heat production parameters. The base of the lithosphere is the 1300 °C isotherm and is a boundary condition. The surface temperature of the model is also a fixed value boundary condition, which is taken as 11°C for Ireland based on Goodman et al., (2004). The detailed description of the methods used in this study can be found in Chambers et al., (2023) and Fullea et al., (2021), and are briefly summarised here along with the input datasets.

3.1 Data

To produce detailed subsurface temperature maps across Ireland, multiple input datasets across the island are required (Figure 1). The temperature maps are produced as a series of points at a lateral resolution of 0.2° x 0.2°, which is the minimum lateral resolution allowed by the surface-wave data produced by Chambers et al., (2023). Each point requires information on the Rayleigh and Love surface-waves, elevation, Moho depth, surface heat flow, thermal conductivity and radiogenic heat production, produced by previous studies which are briefly described below.

3.1.1 Surface waves

The surface wave dataset was created from recent large scale deployments of broadband seismometers across Ireland using the permanent Irish National Seismic Network (INSN, www.insn.ie) (Blake et al., 2012; INSN, 1993) and Great Britain Seismograph Network (Baptie, 2018) stations, and temporary

networks including Ireland Array (Lebedev et al., 2012; Lebedev & The Ireland Array Working Group, 2022), the Dublin Basin temporary network (Licciardi et al., 2014), WaveObs (Möllhoff & Bean, 2016), ISLE and ISUME (Do et al., 2006; Landes et al., 2004, 2007; O'Donnell et al., 2011; Polat et al., 2012; Wawerzinek et al., 2008), the SIM-CRUST project (Piana Agostinetti & Licciardi, 2015) and Blacknest (Blacknest, 2020). Data from 2010 to 2020 were focussed on, in order to maximise coverage across Ireland because the surface-waves were computed using pairs of stations present concurrently (Bonadio et al., 2021; Chambers et al., 2023).

3.1.1.1 Rayleigh-waves

The Rayleigh-wave phase velocity maps are from Bonadio et al., (2021). They were computed using data from the networks listed above, and were originally produced on a triangular grid. For each point in the regional grid used in the joint inversion of this study, the closest point in the Rayleigh-wave phase velocity maps was determined and the corresponding phase velocity dispersion curve was extracted.

3.1.1.2 Love-waves

The Love-wave dispersion curves and phase velocity maps used in this study are those produced by Chambers et al., (2023). These again used data from the seismic networks listed above and are at the chosen grid resolution of this study (0.2° x 0.2°, Figure 1a). A dispersion curve was extracted for each point from the dispersion maps at different periods (Figure 1e).

3.1.2 Elevation

Elevation data were taken from ETOPO1 (Amante & Eakins, 2009) (Figure 1a). For each point at the 0.2° x 0.2° resolution in this study, the average of all points within a 10 km radius was taken and an uncertainty ± 10 m is assigned in the inversion. .

3.1.3 Moho depth

The input Moho depth is taken from a combination of Bonadio et al., (2021) and Licciardi et al., (2014), 2020). Bonadio et al., (2021) used Rayleigh surface waves to infer the Moho depth while Licciardi et al., (2014, 2020) determined Moho depth from receiver functions and reflection and refraction seismic data (Landes et al., 2005), which are more direct estimates of Moho depth. Both models are broadly similar in the large-scale structures, and hence we use an average of both models in this work. The Moho models were regridded to the 0.2° x 0.2° used for the temperature models here, and the average of the two models was taken at each point, which in most instances was the same due to the similarity of the models. The Moho depth has an associated uncertainty of ± 2 km accounting for variations in the model (Figure 1f) and to match the upper end of uncertainty as determined by Licciardi et al., (2020). This parameter is inverted for in the joint geophysical-petrological inversion.

3.1.4 Surface Heat Flow (SHF)

Surface heat flow was taken from Mather et al., (2018) who interpolated 22 paleoclimate corrected heat flow estimates for the island of Ireland. Values were subsequently interpolated at each point on the 0.2° x 0.2° grid. The SHF assigned uncertainty is ± 5 mWm^{-2} (Figure 1b).

3.1.5 Thermal property data

3.1.5.1 Thermal conductivity (TC)

TC values were taken from the map in Chambers et al., (2023) where a total of 122 TC measurements from different studies (Brock, 1989; Brock & Barton, 1987; Long et al., 2018; Mather et al., 2018; ShallowTHERM, 2021), varying in location, depth and lithology, were assigned to 19 broad lithological units. Here, an average value from each group of TC values was used for each lithological unit together with an uncertainty estimate (Table 2). Values for TC were taken at each point on the 0.2° x 0.2° grid (Figure 1c).

3.1.5.2 Radiogenic Heat Production (RHP)

Radiogenic heat production (RHP) is both an input parameter and inversion parameter. Values of RHP from the sediments/upper crust are taken from the map of Willmot Noller & Daly, (2015) at each point on the 0.2° x 0.2° grid (Figure 1d) and assigned to a specific lithology based on the GSI bedrock geology map (Geological Survey Ireland, 2020). This is used as a prior value for the average RHP of the whole crust as the inversion only takes one value for crustal RHP (inversion variable) and is updated during each iteration of the inversion. There is minimal damping on this parameter allowing it to freely vary as described in Chambers et al., (2023). In future updates to the inversion code, assigning RHP to individual layers will be implemented.

To automate the procedure, all of the datasets were gridded at the same lateral spacing as the final temperature maps.

3.2 Joint Geophysical-Petrological Inversion

The inversion is performed on 1D vertical columns (Located on Figure 2) due to the sensitivity of the input datasets being primarily to Earth's 1D lithospheric structure, and no explicit lateral regularisation is considered. . In contrast to Chambers et al., (2023) where six 1D columns with the most reliable geophysical, petrophysical and thermal input data were inverted, this study inverts data in a 0.2° x 0.2° lateral resolution grid across Ireland (703 columns in total) to produce laterally continuous temperature models, necessary for quantifying geothermal potential across the island.

A 3-layer crust, with a prior 10 km thickness for each layer, was used, which is a reasonable assumption in Ireland based on previous geophysical and geological studies (e.g. Gómez-García et al., 2023; Hauser et al., 2008; Landes et al., 2005; Licciardi et al., 2020; O'Reilly et al., 2010, 2012). A Vp/Vs value for each layer was assigned based on Hauser et al., (2008). The damping parameters for density, crustal thickness, shear-velocity and radial anisotropy were tested in Chambers et al., (2023) (Table 1) and were kept the same for this study.

The seismic surface-wave phase-velocities were calculated using MINEOS (Masters et al., 2007) with an averaged reference shear-velocity, density and thickness assigned for each layer in the mantle, calculated from the reference model BL21 (Bonadio et al., 2021) and a 10 km thick layer for the upper, mid and lower crust as described above. Vertical gradient damping was applied to the radial anisotropy when inverting for shear-wave velocity to allow velocity to change smoothly with depth. For density, a reference model of 2750, 2900, 3050 kg/m^3 for the upper, middle and lower crust was used based on Fullea et al., (2014). The inversion model was discretised in 2 km depth increments for temperature, velocity, anisotropy and density.

3.3 Uncertainty Analysis

To determine uncertainty for the final best temperature model, further tests were carried out on nine representative columns. TC (an input parameter) and key inversion variables controlling the temperature distribution (RHP, Moho depth, LAB depth) (Table 1 & Table 2) were fixed to a range of plausible values in the inversion, in order to estimate their uncertainty and the overall trade-off between the parameters. The ranges for each parameter/variable used in the uncertainty analysis are summarised in Table 1. Thermal conductivity was varied for sensible ranges for the expected bedrock geology at each point based on the TC map of Chambers et al., (2023) and the GSI bedrock viewer (Geological Survey Ireland, 2020) (Table 2). The nine columns were selected based on the availability of reliable constraining data. This included locations with direct temperature measurements and SHF values calculated from the borehole TC. The columns in Mallow and Co. Donegal, were selected due to the presence of warm springs and granite bodies, respectively, rather than from the input data.

The procedure is as follows: for each of the 9 columns additional inversions were run fixing the key input parameter/inversion variables while the rest of the variables were free to vary and inverted for as normal (Table 1 & Table 2).

While the selected parameters are the ones that most affect our crustal temperatures in the inversion, these parameters are also correlated with one another. Therefore fixing all parameters independently of each other will likely select combinations of output models that do not make sense physically. Varying all key parameters/variables together within sensible ranges is also computationally expensive so another uncertainty test was run where only one parameter/variable was kept fixed at a time and changed for each inversion while the rest were inverted for as normal. The results indicate that the minimum and maximum temperature range is larger at lithospheric depths when every key input parameter/variable is kept fixed for each inversion and allowed to change between inversions, as expected. The RMS and STD are smaller when just one parameter/variable is changed (Figure 8 and Supplementary Figure 2). However, the best model and the mean models all fall within the STD bands for both tests. We proceed with the tests varying 1 parameter/variable for several reasons. First, the parameters are correlated with one another in the inversion meaning changing 1 parameter will modify the output of another, which can't happen if we fix the variables. This produces unrealistic models which arbitrarily increase the uncertainty. Also modifying all variables is compute intensive. We conclude running uncertainty tests where only one parameter/variable is modified at a time, is representative for the full inversion and is sufficient to produce reliable uncertainty plots at every point in our model for the 0.2° x 0.2° grid (Figure 6 & Figure 7).

Once all possible inversions had been run, we inspected the output data misfit parameter for both tests. The data misfit parameter is the average misfit from all the inversion variables including SHF, phase velocity, RHP etc. (Figure 8) and further information can be found in Fullea et al., (2021),Section 5.1). The spread of the data misfit was analysed and the misfit ratio (misfit new model / misfit best temperature model) were compared. Based on the distribution of the output models, a misfit ratio of 1.05 was chosen. This allowed us to keep a sufficient number of models to assess uncertainty while removing those that are unrealistic.

The overall uncertainty of the accepted models is then calculated as the RMS of the difference between the acceptable output temperature models T_m, and the best temperature model T_i:

$$RMS = \sqrt{\overline{(T_i - T_m)^2}}$$

In addition to the 9 locations used for testing uncertainty, inversions were performed at every point in the 0.2° x 0.2° grid by changing one input parameter/variable within a range of plausible values and keeping this value fixed for the inversion, (Table 1 & Table 2). Points that were in the sea were removed as the input datasets cover the land area only. Additionally, columns that were predominantly offshore were removed as our parameterisation of the inversion requires onshore crust with positive elevation. Models with a misfit >5% larger than the original best model were removed (Figure 7).

Parameter	TC (W/(m K))	RHP (μW/m³)	Moho depth (km)	LAB depth (km)
Range	*	± 0.5 (0.1 μW/m³ intervals)	± 5 (1 km intervals)	± 30 (5 km intervals)

*Table 1 Parameter/variable ranges used for the testing of the uncertainty in the temperature models. For parameters with ±, this means the values tested were ± the range from the best model parameters for each point. * Thermal conductivity was varied within specific lithological rages as listed in Table 2 with 0.1 W/(m K) increments.*

	Rock Type	Average TC (W/(m K))	Range TC (W/(m K))
1	Palaeozoic basic intermediate volcanics	1.80	1.80 to 2.10
2	Palaeocene basalt	1.90	1.80 to 2.10
3	Cambrian greywacke, slate and quartzite	2.00	1.90 to 2.10
4	Carboniferous volcanics/ Devonian volcanics/ Ordovician granite/ Silurian-Devonian granite and appinite	2.10	1.90 to 2.20
5	Mesoproterozoic gneiss	2.15	2.05 to 2.35
6	Cretaceous chalk flint glauconitic sandstone	2.20	1.60 to 2.80
7	Mesoproterozoic and Paleoproterozoic Annagh gneiss complex, granitoid orthogneiss	2.27	2.05 to 2.35
8	Ordovician Silurian marine greywacke and mudstone	2.40	2.10 to 2.80
9	Neoproterozoic metasedimentary rocks (Dalradian)	2.50	2.20 to 2.80
10	Silurian-Devonian conglomerate and mudstone (Old Red Sandstone) / Devonian sandstone and mudstone	2.60	2.20 to 3.40
11	Viséan limestone and calcareous shale	2.70	2.30 to 3.10
12	Jurassic mudstone and limestone	2.75	2.30 to 3.10
13	Tournaisian limestone	2.80	2.30 to 3.10
14	Oligocene clay, sand and lignite	2.90	2.70 to 3.40
15	Permian sandstone conglomerate evaporite / Tournaisian sandstone, mudstone and limestone/ Triassic sandstone, mudstone and evaporite	3.00	2.70 to 3.40
16	Ordovician siltstone, sandstone greywacke and conglomerate / Namurian shale, sandstone, siltstone and coal / Silurian marine sandstone, siltstone and conglomerate / Westphalian shale, sandstone, siltstone and coal	3.07	2.60 to 3.40
17	Permian sandstone, conglomerate and evaporite / Tournaisian sandstone, mudstone and limestone / Triassic sandstone mudstone and evaporite	3.10	2.70 to 3.40
18	Viséan sandstone mudstone and evaporite / Silurian deep marine mudstone, greywacke and conglomerate	3.20	2.80 to 3.40
19	Serpentinite and sedimentary melange	3.40	3.20 to 3.40

Table 2 TC ranges for each rock type. The average TC is taken from Chambers et al., (2023). *Lithologies are taken from the GSI bedrock viewer and ranges were from previous measurements of TC in Ireland* (Geological Survey Ireland, 2020).

3.4 Sensitivity Analysis

SHF was not included in the uncertainty analysis as it is input data with associated prior uncertainty. Given the inversion is trying to fit this as data, any modifications to the input datasets that the inversion is trying to fit will cause large changes to the output temperature and is not representative of an actual uncertainty in the resulting models, as we have to assume the input data is correct. However, the SHF map contains, in places, high uncertainty from interpolation between limited data points to make the final input map in the 0.2° x 0.2° grid (Mather et al., 2018). Given the variation in uncertainty for the input SHF values, we also tested the sensitivity of the model when the input SHF is modified.

First, we tested the case of high uncertainty. We increased the uncertainty in the SHF to ±20 mW/m^2, allowing the inversion more freedom to fit the SHF from the original ±5 mW/m^2 (green line Figure 9). The second test was to fix the SHF to a specific value and reduce the uncertainty to near 0 (the inversion requires an uncertainty >0 so we chose 0.0001 to keep this as small as possible). The purpose of this

test is to see how the inversion changes when we have confidence in our input data. Three inversions were then run on each of the 9 columns: 1. with the expected best SHF value (orange line) and 2. & 3. ±20 mW/m^2 difference from this value (blue and red lines)(Figure 9).

4 Results

703 1D columns of Ireland's subsurface were inverted and collated to make a 3D temperature model. The heat conduction equation is parameterised in 2 km depth increments which were interpolated to 1 km spacing (10 m for the depth to the 30, 60 and 90 °C isotherms). The output temperature models range from the surface to 660 km depth but the focus for this paper is from 0 km sea level to the base of the lithosphere (LAB) (Figure 2 and Supplementary Figure 1). For presentation purposes we smooth the models, but the original grid spacing can be seen in Figure 1a.

The new subsurface temperature maps range from <50 to 90 °C at 2 km depth for all of Ireland. The models suggest temperatures are warmest in the north and east of the island (75 to 90 °C at 2 km depth) and in areas with surface granite exposure (>85 °C for the Co. Donegal and Galway granites, and 75 to 80 °C beneath the Leinster and Mourne granites at 2 km depth) (Figure 2). Temperatures are cooler in the south and in the Midlands ranging from <50 to ~70 °C, at 2 km depth.

The geothermal gradient (Figure 5a) is computed from the modelled temperatures at 1 km and 2 km depth and the upper crustal TC value assigned based on lithology. We only average the first km as the gradient is broadly linear for the first 10 kms as shown in Figure 8 and Supplementary Figure 2. The geothermal gradient ranges from <20 °C/km in the south and Midlands, before increasing to > 30 °C/km for the Leinster granite and east coast of Ireland. The geothermal gradient increases northwards to 35 °C/km beneath much of Northern Ireland, reaching a maximum of ~40 °C/km beneath the Donegal and Galway granites (Figure 5a). In addition, the depths to the 30, 60 and 90 °C isotherms were extracted from the 3D temperature volume (Figure 5b-d). These show a similar pattern to the temperature maps with areas of warmer temperature having shallower depths to the isotherms and cooler regions being deeper and having the coolest geothermal gradient, as expected. The depth to the 30 °C isotherm ranges from 450 m to 1.1 km depth whereas the 90 °C is located between 2 and 3.8 km depth (Figure 5).

The output RHP ranges from 0.5 to 2.0 μW/m³ (Figure 4) with the highest values in the northwest beneath the Donegal granite, and in the Iapetus suture zone, extending from county Clare to the Mourne granites. The lowest RHP values are in Co. Galway and the south of the island of Ireland. Moderate RHP values are found beneath the Antrim basalt sequences (~1.0 μW/m³). The area of the Leinster granites have higher RHP than the surrounding rocks by +0.2 μW/m³.

The uncertainty analysis suggests the temperature uncertainty is ~3.5 °C at 2 km depth, presented in Figure 6 & Figure 7. The uncertainty analysis also indicates we have confidence in most areas of our model with low RMS values. Supplementary Figures 3 and 4 show the misfit for 1 column when changing Moho depth and LAB depth, and how the RMS changes based on each fixed input parameter. The largest source of temperature uncertainty in our models is the RHP (average RMS at 2 km depth ~ ± 5 °C), whereas Moho and LAB depth show the lowest contributions (average RMS at 2 km depth of ~ ±1 °C) (Supplementary Figure 4). We also included SHF to show the variation in the RMS if this was included as an inversion parameter rather than data. This produces the highest overall RMS values and we investigated the SHF through a series of sensitivity tests.

The SHF sensitivity tests for increasing the uncertainty produced a reduction in the misfit value and suggest future studies should use a larger uncertainty for SHF data in Ireland. The tests for fixed SHF produced significantly higher misfit values and modified the resulting geotherms significantly (Figure 9 and Supplementary Figure 5). show the requirement to know your data. The temperature at 2 km

depth changed by ±35°C in the most extreme case (Kells) and ±15 °C in the most minor case, and the RHP changed by a maximum of 0.8 μWm^{-3}. These values are a lot higher than the variations we expect from our model and highlight the importance of using the best input data possible and providing a realistic uncertainty value for any input datum.

As independent validation, (Chambers et al., 2023)(Figures 12 & 13) compared modelled temperature from the integrated inversion with measurements in six boreholes, finding that all temperature values were reproduced within ± 2 °C at 2 km depth for RHP and TC ranges based on the local bedrock geology for the upper crust, providing confidence in the models. This is also within the RMS value computed above as shown in Figure 6. Another test carried out at the Tallaght GT1 well found that our model predicted a depth of 900 m to the 30 °C isotherm (model interpolated to 100 m depth increments) with the measured value at 749 m for the 30 °C isotherm (*Personal communication GSI and GeoServ*). Given no prior petrophysical information was used in the inversion at this location, the closeness of fit with our model shows this procedure gives a good starting point for further local scale studies to refine the geothermal gradient.

As a by-product of the thermal modelling we have derived new maps for the depth to the Moho and LAB (Figure 3a & b). The new Moho model ranges from 25 to 33 km, with thicker crust in southern and central Ireland at 30 to 33 km thick, and thinner crust in counties Galway, Mayo, NE Ireland and eastern Co. Donegal (25 to 29 km thick). The crust ranges from <26 km in the northeast of the island, increasing to >32 km in central Ireland with average values of 29.5 km for the island (Figure 3a). The obtained LAB depth (Figure 3b) shows similarities to the Moho depth map with the thickest lithosphere in central Ireland (112 km) and southwest Ireland (108 km), thinning to 76 km in northeast and average values of ~94 km thick. Broadly both the Moho and LAB maps thin from southwest to northeast. Both the LAB and Moho depth maps show a clear change between north and south of the Iapetus Suture Zone with thicker crust and lithosphere south of this boundary and thinner to the north.

5 Discussion

5.1 Temperature models and Radiogenic Heat Production

Temperatures in Ireland range from <50 to 90 °C at 2 km depth (Figure 2 and Supplementary Figure 1). The warmest temperatures are located beneath areas with known granitic intrusions and areas of thinner crust such as the NE of Ireland. At 5 km depth the Galway and Donegal granitic regions exceed 180°C similar to some of the highest temperatures observed in the UK which are being explored for future electricity generation (Abesser et al., 2020).

Most of the RHP values are within the typical ranges for bulk crustal RHP (0.74 $\mu W\ m^{-3}$ to 1.38 $\mu W\ m^{-3}$ (Jaupart et al., 2016; Vilà et al., 2010)). The radiogenic heat production is closely tied to the input SHF with areas of high SHF having high RHP predicted in our models. However, there are some variations such as the Mourne granites which appear to have higher RHP than the SHF map. The RHP in the south of the island is low for continental Phanerozoic terranes (<0.7 $\mu W\ m^{-3}$) and suggests that the low SHF value which comprises only a single data point is potentially inaccurate and additional temperature measurements should be taken. This low SHF and resulting RHP in the south will result in lower temperatures in the model, which in reality may be higher if more realistic crustal RHP values are considered. There are no boreholes in this region to verify the model but it is likely that the temperature could be higher than the models predict due to limited input data.

The granitic regions have high radiogenic heat production both in our output model and in previous studies (Figure 4 & Figure 1d) which would result in elevated temperatures for the models. The RHP is variable for each granitic area, with high RHP beneath the Donegal Granite and moderately elevated

heat production for the Galway and Mourne granites. In contrast, the Leinster granites are ~1.2μW/m³ which is similar to crustal averages for RHP (Jaupart et al., 2016). Similarly, the edges of the Galway granite have some of the lowest RHP in the model. TC is also low in our models for areas with granite, compared to global averages (Cho et al., 2009; Clauser & Huenges, 1995; Long et al., 2018; Somerton, 1992), due to the assigned TC being a combination of granite and other lithologies such as basaltic units which have a low TC. These would potentially be higher if TC had been split into a purely granitic unit which was not the case for (Chambers et al., 2023) who had too few TC measurements on granites from previous studies to make a separate sub-group. Crustal and lithospheric thicknesses are also variable for the individual granitic regions suggesting the radiogenic heat production is the primary driver for the elevated temperatures in these areas.

The Leinster Granite is cooler than the Galway and Donegal granite sequences, suggesting a difference in the composition or thickness. The RHP for this granitic region is also the lowest for the model (Figure 4). Previous studies reported a range of radiogenic heat production rates for the different granites, with the lowest in Leinster (Willmot Noller & Daly, 2015). This would result in cooler temperatures and a lower geothermal gradient, which matches well to the output RHP (Figure 4) and is consistent with the temperature maps in our models (Figure 2). The lateral extent of these bodies will be larger than this model as we take the surface extent of the bedrock geology to be the same for the whole upper crust, resulting in a minimum temperature estimate for the granite. The inversion is also performed on 1D columns which assume no lateral heat flow, though the SHF partly corrects for this by being higher over granitic bodies. The limited measurements for SHF reduce its influence, however (Mather et al., 2018). The subsurface extent from seismic, gravity and electrical resistivity models provides evidence for larger lateral extent than observed in these models (Delhaye et al., 2017, 2019; O'Donnell et al., 2011; O'Reilly et al., 2012; Yeomans, 2011) and therefore our temperature estimates for these areas are likely a lower bound.

The Mourne granites are similar to the Leinster granites and are not hotter than average in this model, unlike the other granitic regions. There are several potential reasons for this. Firstly, the surface extent of the granite has been averaged with mudstone and sandstone layers when selecting a 20 km area, which affects the assigned TC. The SHF data isn't elevated, in contrast to the Galway and Donegal granites, which would also result in lower temperatures in the model. Previous studies of Irish granites have found compositional differences between the granites of the Mourne Mountain Complex and the Galway, Donegal and Leinster granites and this is reflected in the measured SHF (Mather et al., 2018). The latter granites are more acidic and are visible as negative gravity anomalies, in contrast to the Mourne granites which have a positive gravity anomaly signature and have been associated with the presence of a denser mafic body located beneath the exposed granitic rocks (Reay, 2004; Yeomans, 2011). Given the high shallow RHP (some of the highest values in Ireland (Willmot Noller & Daly, 2015)), it is likely this area is warmer than our model suggests or is volumetrically small and shallow.

The Antrim Lava Group in Northern Ireland is located on top of some of the warmest temperatures of the model. Previous studies suggest this area has low surface heat flow (Mather et al., 2018) and the thermal conductivity of this unit is low, <2.0 W/(m K) (Chambers et al., 2023; Gebski et al., 1987; Raine & Reay, 2019; Wheildon et al., 1985). Similarly the RHP is low to moderate in the model (Figure 4). The basalt sequences range from 10's to 100's of meters thick (Delhaye et al., 2017, 2019; Raine & Reay, 2019) and these overlie more thermally conductive and radiogenic limestone and sandstone units (English et al., 2023; English et al., 2022; Raine & Reay, 2019). Therefore, the basalt units are likely acting as an insulating layer (cap rock), trapping heat rising from the mantle in a sandstone geothermal reservoir characterized by a thin and hot lithosphere.

The coolest areas in our model are in the Midlands and the southwest of the island (<52 °C at 2 km depth, Figure 2). The Midlands of Ireland were modified during the Caledonian orogeny which left a thickened lithosphere with respect to the surrounding Irish terranes as an imprint. As the LAB is deeper, the mantle heat source is farther from the surface resulting in cooler geotherms as observed in this work and Chambers et al., (2023). A potentially surprising cool region is Mallow, Co. Cork (Figure 2, bottom right panel, indicated by an M). It is an area with thick lithosphere and there are extensive carbonate sequences which have a lower TC than the granites (Chambers et al., 2023; Long et al., 2018) and SHF & RHP measurements for the area are relatively low (Mather et al., 2018; Willmot Noller & Daly, 2015) which agree with the temperature models that this is a relatively cool region. However, this area is known for its warm springs and is already using geothermal heat from the warm springs to heat a swimming pool, suggesting the geothermal potential of an area is closely related to the ability to bring heat from depth up to the surface. Deep penetrating faults to allow fluid circulation are known in this area (Meere & Banks, 1997). Therefore, while our model suggests at 2 km depth, temperatures are everywhere sufficient for heating (60 °C for heating and >150°C for electricity generation (DECC, 2020, 2024)). Future studies should focus on the availability of fluids and fluid pathways that bring heat to the surface which is an in progress part of the DIG project.

5.2 Geothermal Gradient

The geothermal gradient ranges from <20 °C/km to ~40 °C/km in the upper crust (Figure 5). In Northern Ireland where there are some of the highest gradients (>30 °C/km), formation fluids should be suitable for large-scale direct heating uses (Pasquali et al., 2010, 2015; Raine & Reay, 2019). These gradients are close to those in Southampton, and for the United Downs and Eden Geothermal deep geothermal projects in southwestern GB (Beamish & Busby, 2016; Farndale et al., 2022). The geothermal gradients we observe in Northern Ireland are significantly higher than the previously estimated averages for the area (Beamish & Busby, 2016; Busby, 2014; Busby et al., 2011; Farndale et al., 2022; Parkes et al., 2020; Raine & Reay, 2019; Wheildon et al., 1985).

At 2 to 3 km depth temperatures would be sufficient for combined heat and power generation, with the Rathlin Basin, Larne Basin, Lough Neagh Basin, western Donegal Granite and Galway Granite being the best candidates for this combined deep geothermal use. Previous studies suggested the Rathlin Basin would have the highest geothermal gradient when compared to Lough Neagh and Larne basins. However, the original geothermal gradients were calculated on temperature data taken directly after drilling as bottom hole temperature measurements, when the temperatures were likely cooler due to circulating mud (Pasquali et al., 2010, 2015; Raine & Reay, 2019). The geothermal gradient determined by our model of ~35 °C/km from the Ballinlea-1 well in the Rathlin Basin (English et al., 2023; English et al., 2022), is consistent with the previous studies suggesting the higher geothermal gradients at Lough Neagh (35 °C/km) and Larne (38.5 °C/km) are likely correct and significantly higher than the previous 32 and 28 °C/km suggested (Pasquali et al., 2010). In any case, areas with the lowest geothermal gradients would still be sufficient for heating purposes as evidenced in Mallow.

5.3 LAB and Moho depth

The new LAB depth derived in this study (Figure 3b), ranges from 76 to 112 km deep. The new model suggests thicker lithosphere in southern, central and eastern Ireland which trends northwest – southeast. South of the Iapetus Suture Zone the LAB is deeper while to the north, the LAB is shallower. This thinning of the lithosphere from southwest to northeast may indicate the boundary between the Avalonian and Laurentian domains when the two supercontinents collided during the Caledonian orogeny. This is consistent with previous studies of seismic data and geological evidence (Bonadio et al., 2021; Chew & Stillman, 2009; Fullea et al., 2014; A. G. Jones et al., 2014). In contrast, Landes et al.,

(2007) didn't find a thicker lithosphere beneath the Iapetus Suture Zone, though this may be due to a sparse input dataset producing smooth models capturing only the first order south to north lithospheric thinning trend.

Previous estimates of LAB depth are variable, with depths of 55 to 85 km for a S-to-P receiver function study (Landes et al., 2007), 85 to 145 km thick from a joint modelling of gravity, magnetic and elevation data with a seismically derived Moho depth (Baykiev et al., 2018) and 95 to 105 km when the Moho was constrained by gravity rather than seismic data in the same study. 1D surface wave models for Ireland suggest the LAB ranges from 60 to 100 km depth in Ireland (Bonadio et al., 2021; Lebedev et al., 2024). The work of Landes et al., (2007) suggested the LAB was anomalously shallow everywhere in Ireland, either from thinning by thermal erosion from the proto-Icelandic plume head or from Ireland being the transition from oceanic to continental crust, though this boundary is expected far offshore to the west of Ireland. A joint inversion using gravity, elevation and mantle compositions produced an LAB map ranging from 85 km thick in the north increasing to 115 km in the south, consistent with the model shown here. The Landes et al. (2007) model required a minimum lithospheric thickness of 85 km, otherwise topographic variations could not be reconciled (Jones et al., 2014). The model shown here has more detail and is less smooth than previous studies, which is due to the larger volume of input seismic data used in the inversions allowing us to more accurately map the lithospheric boundary.

The thinnest lithosphere of the model is in the north of the island where the Antrim Lava Sequence is located and in the east beneath Belfast and the Strangford Lough region. The extensive volcanic sequences in the area suggest the lithosphere could have been thinned during their emplacement which previous studies have suggested was from thermal erosion in the past from the Icelandic plume (Bonadio et al., 2021; Landes et al., 2007).

The new Moho map ranges from 25 to 33 km depth (Figure 3a) and shows similar trends to the LAB map suggesting comparable origins. The Moho map is similar to previous seismic and joint inversion models with greater detail and some differences (Baykiev et al., 2018; Bonadio et al., 2021; Fullea et al., 2014; Jones et al., 2014; Licciardi et al., 2014, 2020).

The thinnest crust is in the north and west of the island. In Northern Ireland this thin crust coincides with an area with known warm temperatures from the Portmore (Figure 8) and Ballinlea-1 boreholes (Chambers et al., 2023). The elevated temperature in these boreholes reflects both the lithology (porous sandstone with a high TC, capped with a low TC basalt) and this study suggests these temperatures are also high due to the thin lithosphere. In addition, given the thin Moho occurs beneath the Antrim Lava Sequence, the shallower Moho depths likely reflect thinning induced by the Icelandic plume (Bonadio et al., 2021) and/or crustal extension of the Larne and Rathlin basins (Landes et al., 2005; O'Reilly et al., 2010). A shallower Moho is also observed towards the west in Connemara and Mayo which is visible on the input Moho map (Figure 1). Given limited evidence for basin extension or volcanic intrusive centres in this area, it is possible the thinner crust present in the input data is influencing the output.

The deepest Moho is observed in central and southern Ireland following the broad trend of the Iapetus Suture Zone. We attribute this thickened crust to compression during the collision of the Avalonian and Laurentian terranes. Moho depths from Ireland derived from gravity data and isostatic modelling suggest the Moho is 27 to 30.5 km deep (Baykiev et al., 2018) showing a smoothed pattern at odds with our results. However, when crustal seismic data (controlled source and receiver functions) was included the jointly inverted Moho ranges from 27 to 34 km, which is more similar to our model results (25 to 33 km).The new state-of-the-art LAB and Moho depth maps provide fundamental information for future studies investigating the tectonic evolution of the island and its geothermal and mineral resources.

To improve the temperature models in the future, more refined crustal thermal property data should be used at a finer grid spacing, while keeping the surface wave data at the same resolution. For example, TC changes with lithology and could be varied at a finer resolution than the seismic datasets which are constrained to their own resolution. This would allow better matches to measured geothermal gradients in regions where there are rapid changes in lithology. In addition, better knowledge of the subsurface, including the depth extent of lithological units could be gained by utilising new gravity and MT datasets being gathered and processed in Ireland (Kiyan et al., 2023). This would improve assignment of thermal properties and crustal geometries and hence improve the robustness of the temperature model. These datasets should then be combined with a multi-layer crustal inversion, including sediment layers and additional gravity data constraints in a 3D framework, able to account for lateral heat flow. Finally, the thermal conductivity ranges were based on an averaged model for each rock type based on limited Irish rock measurements. More TC measurements should be taken, and the full range of values tested rather than an average for each lithological unit. Finally, more deep temperature measurements in deep boreholes are required to ground truth and improve the models

6 Conclusions

In this paper new subsurface temperature (Figure 2) maps with uncertainty have been computed for Ireland based on joint geophysical-petrological inversion of surface wave, SHF and petrophysical data sets. The models have also been verified by comparison with direct borehole temperature measurements where possible. The addition of uncertainty to the final temperature models provides a reliable resource that can be used for risk analysis in developing future projects and further exploration as uncertainty allows a definition of risk. The temperature and geothermal gradient maps (Figure 5) indicate a higher geothermal gradient for Ireland than previously reported, suggesting temperatures everywhere at 2 km depth are sufficient for residential and industrial heating purposes. The warmest areas in Ireland according to our models coincide with granites and the Antrim Lava Sequence. The hottest granites are in counties Donegal and Galway and likely reflect higher amounts of radiogenic elements compared to the Mourne and Leinster granites.

New high resolution LAB and Moho depth (Figure 3) maps have been produced with the most up-to-date geophysical data and are the current state of the art with more detail than previous models. The coolest areas in the Iapetus Suture Zone and south of Ireland are also the areas with the thickest crust and lithosphere in our models. This thickening in the Iapetus Suture Zone is likely the result of the collision between Avalonia and Laurentia. Areas with thinner lithosphere typically have warmer temperatures. The Moho depth map also has areas of thinned crust in the north of the island, particularly beneath the Antrim Lava sequence and the Larne and Rathlin basins, suggesting extension has thinned the crust along with thermal erosion from a past mantle plume.

New maps of crustal RHP from our inversion correlate well to the temperature maps suggesting, in general, areas with thicker crust have higher RHP, which may reflect more felsic crustal compositions in the midlands. Similarly, the RHP map shows variations within the granitic areas suggesting areas with higher SHF and consequently RHP are likely to have warmer temperatures such as in Co. Donegal and Galway.

This work shows how parameterising the crust in great detail allows us to scale the workflow for a whole region. This was possible by having large datasets used as input parameters/variables which were available as grids for the region. The uncertainty analysis is specifically tailored to shallow temperature estimates making it useful for the geothermal community and allows assessment of risk for the final temperature models. Future studies could utilise the workflow for areas with similar sparse datasets enabling a better understanding of the geothermal potential and determining areas suitable for further

exploration and exploitation. This will be essential in the near future for energy self-sufficiency, meeting green energy targets and moving to green energy sources.

7 Acknowledgements

We thank GSI and GSNI for providing access to geological maps, thermal conductivity data and for fruitful discussions. The DIG project is funded by the Sustainable Energy Authority of Ireland and Geological Survey Ireland under the SEAI Research, Development & Demonstration Funding Programme 2019 (grant number 19/RDD/522). ELC is funded under the SFI-IRC Pathway Programme 22/PATHS/10676 and the SEAI Research and Development & Demonstration Funding Programme 2022, Grant number 2022/RDD/782. JF is supported by projects PID2020-114854GB-C22 and CNS2022-135621 funded by the Spanish Ministry of Science and Innovation, Additional support from Project InnerSpace (https://projectinnerspace.org) is gratefully acknowledged. We gratefully acknowledge the support of the iCRAG Centre, which is funded by SFI grants 13/RC/2092 and 13/RC/2092_P2 and cofunded under the European Regional Development Fund. Heat Production Rate data were acquired during the IRETHERM project, which was funded by Science Foundation Ireland (grant number 10/IN.1/I3022). Additional support from the UK Natural Environment Research Council Grant Number XE/X000060/1 and the Science Foundation Ireland (SFI) Grant Number 16/IA/4598, cofunded by the Geological Survey of Ireland and the Marine Institute, is acknowledged.

Data Availability Statement

The final Temperature model, uncertainty maps, LAB and Moho maps will be available on the DIAS Access to Institutional Repository (DAIR) with an associated DOI. We are in the process of registering the dataset and will update the manuscript once this is available. https://dair.dias.ie/.

8 References

Abesser, C., Busby, J. P., Pharaoh, T. C., Bloodworth, A. J., & Ward, R. S. (2020). *Unlocking the potential of geothermal energy in the UK Decarbonisation and Resource Management Programme*.

Afonso, J. C., Fernàndez, M., Ranalli, G., Griffin, W. L., & Connolly, J. A. D. (2008). Integrated geophysical-petrological modeling of the lithosphere and sublithospheric upper mantle: Methodology and applications. *Geochemistry, Geophysics, Geosystems*, *9*(5). https://doi.org/10.1029/2007GC001834

Amante, C., & Eakins, B. W. (2009). ETOPO1 1 Arc-Minute Global Relief Model: Procedures, Data Sources and Analysis. *NOAA Technical Memorandum NESDIS NGDC-24. National Geophysical Data Center, NOAA.* https://doi.org/10.7289/V5C8276M

Anikiev, D., Lechel, A., Laura Gomez Dacal, M., Bott, J., Cacace, M., & Scheck-Wenderoth, M. (2019). A three-dimensional lithospheric-scale thermal model of Germany. *Advances in Geosciences*, *49*, 225–234. https://doi.org/10.5194/adgeo-49-225-2019

Axelsson, G., Gunnlaugsson, E., Jónasson, T., & Ólafsson, M. (2010). Low-temperature geothermal utilization in Iceland - Decades of experience. *Geothermics*, *39*(4), 329–338. https://doi.org/10.1016/j.geothermics.2010.09.002

Baptie, B. J. (2018). *Earthquake Seismology 2017/2018 Open Report OR/18/029*. http://earthquakes.bgs.ac.uk/publications/annual_reports/2018_29th_annual_report.pdf

Baykiev, E., Guerri, M., & Fullea, J. (2018). Integrating gravity and surface elevation with magnetic data: Mapping the curie temperature beneath the british isles and surrounding areas. *Frontiers in Earth Science*, *6*(October), 1–19. https://doi.org/10.3389/feart.2018.00165

Beamish, D., & Busby, J. (2016). The Cornubian geothermal province: heat production and flow in SW England: estimates from boreholes and airborne gamma-ray measurements. *Geothermal Energy*, *4*(1). https://doi.org/10.1186/s40517-016-0046-8

Békési, E., Lenkey, L., Limberger, J., Porkoláb, K., Balázs, A., Bonté, D., Vrijlandt, M., Horváth, F., Cloetingh, S., & van Wees, J. D. (2018). Subsurface temperature model of the Hungarian part of the Pannonian Basin. *Global and Planetary Change*, *171*, 48–64. https://doi.org/10.1016/J.GLOPLACHA.2017.09.020

Békési, E., Struijk, M., Bonté, D., Veldkamp, H., Limberger, J., Fokker, P., Vrijlandt, M., van Wees, J.-D., & Fokker, P. A. (2020). An updated geothermal model of the Dutch subsurface based on inversion of temperature data. *Geothermics*, *88*, 101880. https://doi.org/10.1016/j.geothermics.2020.101880ï

Blacknest, A. (2020). *Awe blacknest*. https://www.awe.co.uk/about-us/our-locations

Blake, S., Henry, T., Moore, J. P., Murray, J., Campanyà, J., Muller, M. R., Jones, A. G., Rath, V., Walsh, J., & Blake, S. (2021). *Characterising thermal water circulation in fractured bedrock using a multidisciplinary approach : a case study of St . Gorman ' s Well , Ireland*.

Blake, S., Henry, T., Muller, M. R., Jones, A. G., Moore, J. P., Murray, J., Campanyà, J., Vozar, J., Walsh, J., & Rath, V. (2016). Understanding hydrothermal circulation patterns at a low-enthalpy thermal spring using audio-magnetotelluric data: A case study from Ireland. *Journal of Applied Geophysics*, *132*, 1–16. https://doi.org/10.1016/j.jappgeo.2016.06.007

Blake, S., Henry, T., Murray, J., Flood, R., Muller, M. R., Jones, A. G., & Rath, V. (2016). Compositional multivariate statistical analysis of thermal groundwater provenance: A hydrogeochemical case study from Ireland. *Applied Geochemistry*, *75*, 171–188. https://doi.org/10.1016/j.apgeochem.2016.05.008

Blake, T., Lebedev, S., O'Reilly, B. M., Agostinetti, N., Agius, M. R., & Schaeffer, A. J. (2012). An unusual occurrence of a moderately sized earthquake (Ml 4.2) on the Irish continental shelf and passive margin. *AGU Fall Meeting Abstracts*, *2012*, S53A-2476.

Bonadio, R., Lebedev, S., Meier, T., Arroucau, P., Schaeffer, A. J., Licciardi, A., Agius, M. R., Horan, C., Collins, L., O'Reilly, B. M., & Readman, P. W. (2021). Optimal resolution tomography with error tracking and the structure of the crust and upper mantle beneath Ireland and Britain. *Geophysical Journal International*, *226*(3), 2158–2188. https://doi.org/10.1093/gji/ggab169

Brock, A. (1989). Heat flow measurements in Ireland. *Tectonophysics*, *164*(2–4), 231–236. https://doi.org/10.1016/0040-1951(89)90016-4

Brock, A., & Barton, K. J. (1987). *Equilibrium Temperature and Heat Flow Measurements in Ireland*.

Busby, J. (2014). Geothermal energy in sedimentary basins in the UK. *Hydrogeology Journal*, *22*(1), 129–141. https://doi.org/10.1007/s10040-013-1054-4

Busby, J., Kingdon, A., & Williams, J. (2011). The measured shallow temperature field in Britain. *Quarterly Journal of Engineering Geology and Hydrogeology*, *44*(3), 373–387. https://doi.org/10.1144/1470-9236/10-049

Cammarano, F., Goes, S., Vacher, P., & Giardini, D. (2003). Inferring upper-mantle temperatures from seismic velocities. *Physics of the Earth and Planetary Interiors*, *138*(3–4), 197–222. https://doi.org/10.1016/S0031-9201(03)00156-0

Campanyà, J., Jones, A. G., Vozár, J., Rath, V., Blake, S., Delhaye, R., & Farrell, T. (2015). Porosity and Permeability Constraints from Electrical Resistivity Models: Examples Using Magnetotelluric Data. In *Proceedings World Geothermal Congress*. www.iretherm.ie

Chambers, E. L., Bonadio, R., Fullea, J., Lebedev, S., Xu, Y., Kiyan, D., Bean, C. J., Meere, P. A., Mather, B., & O'Reilly, B. M. (2023). Determining Subsurface Temperature and Lithospheric Structure form Joint Geophysical-Petrological Inversion: A case study from Ireland. *Tectonophysics*.

Chew, D. M., & Stillman, C. J. (2009). Late Caledonian orogeny and magmatism. In C. H. Holland & I. S. Sanders (Eds.), *The Geology of Ireland* (Vol. 2, pp. 143–173).

Cho, W. J., Kwon, S., & Choi, J. W. (2009). The thermal conductivity for granite with various water contents. *Engineering Geology*, *107*(3–4), 167–171. https://doi.org/10.1016/j.enggeo.2009.05.012

Clauser, C., & Huenges, E. (1995). Thermal Conductivity of Rocks and Minerals. *Rock Physics and Phase Relations: A Handbook of Physical Constants*, *3*, 105–126.

Cloetingh, S. A. P. L., van Wees, J. D., Ziegler, P. A., Lenkey, L., Beekman, F., Tesauro, M., Förster, A., Norden, B., Kaban, M., Hardebol, N., Bonté, D., Genter, A., Guillou-Frottier, L., Ter Voorde, M., Sokoutis, D., Willingshofer, E., Cornu, T., & Worum, G. (2010). Lithosphere tectonics and thermo-mechanical properties: An integrated modelling approach for Enhanced Geothermal Systems exploration in Europe. In *Earth-Science Reviews* (Vol. 102, Issues 3–4, pp. 159–206). https://doi.org/10.1016/j.earscirev.2010.05.003

Cooper, M. R. (2004). Antrim Lava Group, Palaeogene extrusive igneous rocks, Northern Ireland. In W. I. Mitchell (Ed.), *The Geology of Ireland*. Geological Survey of Northern Ireland.

Cooper, M. R., Anderson, H., Walsh, J. J., van Dam, C. L., Young, M. E., Earls, G., & Walker, A. (2012). Palaeogene alpine tectonics and icelandic plume-related magmatism and deformation in Northern Ireland. *Journal of the Geological Society*, *169*(1), 29–36. https://doi.org/10.1144/0016-76492010-182

Cooper, M. R., Crowley, Q. G., & Rushton, A. W. A. (2008). New age constraints for the Ordovician Tyrone Volcanic Group, Northern Ireland. *Journal of the Geological Society*, *165*, 333–339. https://www.lyellcollection.org

Daly, J. S. (2009). Precambrian. In C. H. Holland & I. S. Sanders (Eds.), *The Geology of Ireland* (2nd ed.). Dunedin Academic Press.

DECC, D. of T. E. C. and C. (2020). *Geothermal Energy in Ireland. A roadmap for a policy and regulatory framework*. www.decc.gov.ie

DECC, D. of T. E. C. and C. (2024). *Climate Action Plan 2024*.

Delhaye, R., Rath, V., Jones, A. G., Muller, M. R., & Reay, D. (2017). Correcting for static shift of magnetotelluric data with airborne electromagnetic measurements: A case study from Rathlin Basin, Northern Ireland. *Solid Earth*, *8*(3), 637–660. https://doi.org/10.5194/se-8-637-2017

Delhaye, R., Rath, V., Jones, A. G., Muller, M. R., & Reay, D. (2019). Quantitative geothermal interpretation of electrical resistivity models of the Rathlin Basin, Northern Ireland. *Geothermics*, *77*, 175–187. https://doi.org/10.1016/j.geothermics.2018.09.012

Dewey, J. F., & Strachan, R. A. (2002). Caledonides of Britain and Ireland. *EUROPE/Caledonides of Britain and Ireland*, *2000*, 269–276.

DfE. (2021). *Policy Statement for Geothermal Energy for a Circular Economy Natura Impact Statement Natura Impact Statement*.

Do, V. C., Readman, P. W., O'Reilly, B. M., & Landes, M. (2006). Shear-wave splitting observations across southwest Ireland. *Geophysical Research Letters*, *33*(3), 2–5. https://doi.org/10.1029/2005GL024496

Downing, R. A., & Gray, D. A. (1985). *Geothermal Energy: The potential in the United Kingdom*.

Downing, R. A., & Gray, D. A. (1986). Geothermal resources of the United Kingdom. *Journal of the Geological Society*, *143*(3), 499–507. https://doi.org/10.1144/gsjgs.143.3.0499

English, J. M., English, K. L., Dunphy, R. B., Blake, S., Walsh, J., Raine, R., Vafeas, N. A., & Salgado, P. R. (2023). An overview of deep geothermal energy and its potential on the island of Ireland. *First Break*, *41*(2), 33–43. https://doi.org/10.3997/1365-2397.fb2023009

English, K., English, J. M., Dunphy, R., Blake, S., Walsh, J., Raine, R., Vafeas, N. A., & Rodriguez-Salgado, P. (2022). Deep Geothermal Potential on the Island of Ireland. *3rd EAGE Global Energy Transition Conference & Exhibition*, 1–5. https://doi.org/10.3997/2214-4609.202221086

European Council. (2014). *2030 Climate and Energy Policy Framework*.

Farndale, H., Law, R., & Beyon, S. (2022). An Update on the United Downs Geothermal Power Project, Cornwall, UK. *European Geothermal Congress, Berlin, Germany*.

Farrell, T., Rath, V., Feely, M., Muller, M., Jones, A. G., & Brock, A. (2015). IRETHERM: The Geothermal Energy Potential of Radiothermal Granites in a Low-Enthalpy Setting in Ireland from Magnetotelluric Data. *Proceedings World Geothermal Congress*, 19–25. https://www.researchgate.net/publication/283730888

Fellgett, M., & Monaghan, A. A. (2024). *User Guide: BGS UK Geothermal Catalogue first digital release, legacy data*. https://doi.org/https://doi.org/10.5285/05569 ed5-db0e-4587-807c-58e39ee240fa

Förster, A., Fuchs, S., Förster, H. J., & Norden, B. (2021). Ambiguity of crustal geotherms: A thermal-conductivity perspective. *Geothermics*, *89*. https://doi.org/10.1016/j.geothermics.2020.101937

Frey, M., Bär, K., Stober, I., Reinecker, J., van der Vaart, J., & Sass, I. (2022). Assessment of deep geothermal research and development in the Upper Rhine Graben. *Geothermal Energy*, *10*(1). https://doi.org/10.1186/s40517-022-00226-2

Freymark, J., Sippel, J., Scheck-Wenderoth, M., Bär, K., Stiller, M., Fritsche, J. G., & Kracht, M. (2017). The deep thermal field of the Upper Rhine Graben. *Tectonophysics*, *694*, 114–129. https://doi.org/10.1016/j.tecto.2016.11.013

Fridleifsson, G. O., & Elders, W. A. (2005). The Iceland Deep Drilling Project: A search for deep unconventional geothermal resources. *Geothermics*, *34*(3), 269–285. https://doi.org/10.1016/j.geothermics.2004.11.004

Fritschle, T., Daly, J. S., Whitehouse, M. J., Buhre, S., Mcconnell, B., & Team, I. (2015). Geothermal Potential of Caledonian Granites Astride the Iapetus Suture Zone in Ireland and the Isle of Man-Implications for EGS Prospectivity. In *Proceedings World Geothermal Congress*. www.iretherm.ie

Fullea, J., Afonso, J. C., Connolly, J. A. D., Fernàndez, M., García-Castellanos, D., & Zeyen, H. (2009). LitMod3D: An interactive 3-D software to model the thermal, compositional, density, seismological, and rheological structure of the lithosphere and sublithospheric upper mantle. *Geochemistry, Geophysics, Geosystems*, *10*(8), 1–21. https://doi.org/10.1029/2009GC002391

Fullea, J., Lebedev, S., Martinec, Z., & Celli, N. L. (2021). WINTERC-G: mapping the upper mantle thermochemical heterogeneity from coupled geophysical-petrological inversion of seismic waveforms, heat flow, surface elevation and gravity satellite data. *Geophysical Journal International*, *226*, 146–191. https://doi.org/10.1093/gji/ggab094

Fullea, J., Muller, M. R., Jones, A. G., & Afonso, J. C. (2014). The lithosphere-asthenosphere system beneath Ireland from integrated geophysical-petrological modeling II: 3D thermal and compositional structure. *Lithos*, *189*, 49–64. https://doi.org/10.1016/j.lithos.2013.09.014

Gan, Q., Feng, Z., Zhou, L., Li, H., Liu, J., & Elsworth, D. (2021). Down-dip circulation at the united downs deep geothermal power project maximizes heat recovery and minimizes seismicity. *Geothermics*, *96*. https://doi.org/10.1016/j.geothermics.2021.102204

Gebski, J. S., Wheildon, J., & Thomas-Betts, A. (1987). *Investigations of the UK heat flow field (1984-1987)*.

Geological Survey Ireland. (2020). *Bedrock Geology Data and Maps*. https://www.gsi.ie/en-ie/data-and-maps/Pages/Bedrock.aspx

Gómez-García, C., Lebedev, S., Meier, T., Xu, Y., Le Pape, F., & Wiesenberg, L. (2023). Ambient noise autocorrelation scheme for imaging the P-wave reflectivity of the lithosphere. *Geophysical Journal International*, *233*(3), 1671–1693. https://doi.org/10.1093/gji/ggac509

Goodman, R., Jones, G. L., Kelly, J., Slowey, E., & O'Neill, N. (2004). *Geothermal Resource Map of Ireland. Final Report to Sustainable Energy Ireland*.

Graham, J. R., Holland, C. H., & Saunders, A. D. (2009). The geology of Ireland. In *Ordovician of the North* (pp. 43–67).

Hauser, F., O'Reilly, B. M., Readman, P. W., Daly, J. S., & van den Berg, R. (2008). Constraints on crustal structure and composition within a continental suture zone in the Irish Caledonides from shear wave wide-angle reflection data and lower crustal xenoliths. *Geophysical Journal International*, *175*(3), 1254–1272. https://doi.org/10.1111/j.1365-246X.2008.03945.x

Herrington, R. J., Hollis, S. P., Cooper, M. R., Stobbs, I., Tapster, S., Rushton, A., McConnell, B., & Jeffries, T. (2018). Age and geochemistry of the Charlestown Group, Ireland: Implications for the

Grampian orogeny, its mineral potential and the Ordovician timescale. *Lithos*, *302–303*, 1–19. https://doi.org/10.1016/j.lithos.2017.12.012

INSN. (1993). *Irish National Seismic Network (INSN)Operated by the Dublin Institute for Advanced Studies and Supported by the Geological Survey Ireland. International Federation of Digital seismograph networks*.

Jaupart, C., Mareschal, J. C., & Iarotsky, L. (2016). Radiogenic heat production in the continental crust. In *Lithos* (Vol. 262, pp. 398–427). Elsevier B.V. https://doi.org/10.1016/j.lithos.2016.07.017

Johnston, T. P. (2004). Post-Variscan deformation and basin formation, Northern Ireland. In W. I. Mitchell (Ed.), *The Geology of Ireland*. Geological Survey of Northern Ireland.

Jones, A. G., Afonso, J. C., Fullea, J., & Salajegheh, F. (2014). The lithosphere-asthenosphere system beneath Ireland from integrated geophysical-petrological modeling - I: Observations, 1D and 2D hypothesis testing and modeling. *Lithos*, *189*, 28–48. https://doi.org/10.1016/j.lithos.2013.10.033

Jones, G. L., Goodman, R., Pasquali, R., Kelly, J. G., Neill, N. O., & Slowey, E. (2007). The Status of Geothermal Resource Development in Ireland. *European Geothermal Congress*, *June*, 1–3.

Kassa, M., Alemu, A., & Muluneh, A. (2022). Determination of Conrad and Curie point depth relationship with the variations in lithospheric structure, geothermal gradient and heat flow beneath the central main Ethiopian rift. *Heliyon*, *8*(11). https://doi.org/10.1016/j.heliyon.2022.e11735

Kiyan, D., Chambers, E. L., O'Reilly, B. M., Rezaeifar, M., Tomar, G., Ye, T., Fullea, J., Lebedev, S., Bean, C. J., & Meere, P. A. (2022). Geothermal Study of Southern Ireland: DIG Project. *EGU General Assembly*.

Kiyan, D., Hogg, C., Campanya, J., Bean, C. J., Fullea, J., Blake, S. P., Malone-Leigh, J., Gallagher, P. T., Rath, V., Jones, A. G., & Scanlon, R. (2023, April 26). 3-D Magnetotelluric Assessment of the Geo-resources Potential of the Irish Crust . *EGU General Assembly*.

Landes, M., Ritter, J. R. R., Do, V. C., Readman, P. W., & O'Reilly, B. M. (2004). Passive teleseismic experiment explores the deep subsurface of southern ireland. *Eos*, *85*(36). https://doi.org/10.1029/2004EO360002

Landes, M., Ritter, J. R. R., & Readman, P. W. (2007). Proto-Iceland plume caused thinning of Irish lithosphere. *Earth and Planetary Science Letters*, *255*(1–2), 32–40. https://doi.org/10.1016/j.epsl.2006.12.003

Landes, M., Ritter, J. R. R., Readman, P. W., & O'Reilly, B. M. (2005). A review of the Irish crustal structure and signatures from the Caledonian and Variscan Orogenies. In *Terra Nova* (Vol. 17, Issue 2, pp. 111–120). https://doi.org/10.1111/j.1365-3121.2004.00590.x

Lebedev, S., Fullea, J., Xu, Y., & Bonadio, R. (2024). Seismic Thermography. *Bulletin of the Seismological Society of America*. https://doi.org/10.1785/0120230245

Lebedev, S., Horan, C., Readman, P. W., Schaeffer, A. J., Agius, M. R., Collins, L., Hauser, F., O'Reilly, B. M., & Blake, T. (2012). Ireland Array: A new broadband seismic network targets the structure, evolution and seismicity of Ireland and surroundings. *EGU General Assembly Conference Abstracts*, 3615.

Lebedev, S., & The Ireland Array Working Group. (2022). Ireland Array. In *GFZ Data Services*.

Ledésert, B. A., & Hébert, R. L. (2020). How can deep geothermal projects provide information on the temperature distribution in the upper rhine graben? The example of the soultz-sous-forêts-enhanced geothermal system. *Geosciences (Switzerland)*, *10*(11), 1–24. https://doi.org/10.3390/geosciences10110459

Lee, M. K., Brown, G. C., Webb, P. C., Wheildon, J., & Rollin, K. E. (1987). Heat flow, heat production and thermo-tectonic setting in mainland UK. *Journal of the Geological Society*, *144*(1), 35–42. https://doi.org/10.1144/gsjgs.144.1.0035

Lenkey, L., Raáb, D., Goetzl, G., Lapanje, A., Nádor, A., Rajver, D., Rotár-Szalkai, Svasta, J., & Zekiri, F. (2017). Lithospheric scale 3D thermal model of the Alpine–Pannonian transition zone. *Acta Geodaetica et Geophysica*, *52*(2), 161–182. https://doi.org/10.1007/s40328-017-0194-8

Licciardi, A., Agostinetti, N. P., Lebedev, S., Schaeffer, A. J., Readman, P. W., & Horan, C. (2014). Moho depth and Vp/Vs in Ireland from teleseismic receiver functions analysis. *Geophysical Journal International*, *199*(1), 561–579. https://doi.org/10.1093/gji/ggu277

Licciardi, A., England, R. W., Piana Agostinetti, N., & Gallagher, K. (2020). Moho depth of the British Isles: A probabilistic perspective. *Geophysical Journal International*, *221*(2), 1384–1401. https://doi.org/10.1093/gji/ggaa021

Limberger, J., Boxem, T., Pluymaekers, M., Bruhn, D., Manzella, A., Calcagno, P., Beekman, F., Cloetingh, S. A. P. L., & van Wees, J. D. (2018). Geothermal energy in deep aquifers: A global assessment of the resource base for direct heat utilization. *Renewable and Sustainable Energy Reviews*, *82*(October 2017), 961–975. https://doi.org/10.1016/j.rser.2017.09.084

Limberger, J., van Wees, J. D., Tesauro, M., Smit, J., Bonté, D., Békési, E., Pluymaekers, M., Struijk, M., Vrijlandt, M., Beekman, F., & Cloetingh, S. A. P. L. (2018). Refining the thermal structure of the European lithosphere by inversion of subsurface temperature data. *Global and Planetary Change*, *171*, 18–47. https://doi.org/10.1016/j.gloplacha.2018.07.009

Long, M., Murray, S., & Pasquali, R. (2018). Thermal conductivity of Irish rocks. *Irish Journal of Earth Sciences*, *36*, 63–80. https://doi.org/10.3318/ijes.2018.36.63

Maggio, G., Kiyan, D., Bean, C. J., Queralt, P., Delhaye, R., Hogg, C., Mcateer, J., & Blake, S. (2021). The GEO-URBAN Project: Exploring the Geothermal Potential of Dublin City using Electromagnetic and Passive Seismic Methods. *Proceedings World Geothermal Congress*.

Maggio, G., Subašić, S., & Bean, C. J. (2022). Subsurface characterization using passive seismic in the urban area of Dublin City, Ireland. *Geophysical Prospecting*, *70*(8), 1432–1454. https://doi.org/10.1111/1365-2478.13255

Majorowicz, J., Polkowski, M., & Grad, M. (2019). Thermal properties of the crust and the lithosphere–asthenosphere boundary in the area of Poland from the heat flow variability and seismic data. *International Journal of Earth Sciences*, *108*(2), 649–672. https://doi.org/10.1007/s00531-018-01673-8

Masters, G., Barmine, M., & Kientz, S. (2007). *Mineos user's manual*. Computational Infrastructure for Geodynamics.

Mather, B., Farrell, T., & Fullea, J. (2018). Probabilistic Surface Heat Flow Estimates Assimilating Paleoclimate History: New Implications for the Thermochemical Structure of Ireland. *Journal of*

Geophysical Research: Solid Earth, *123*(12), 10,951-10,967. https://doi.org/10.1029/2018JB016555

Mather, B., & Fullea, J. (2019). Constraining the geotherm beneath the British Isles from Bayesian inversion of Curie depth: integrated modelling of magnetic, geothermal, and seismic data. *Solid Earth*, *10*(3), 839–850. https://doi.org/10.5194/se-10-839-2019

Meere, P. A., & Banks, D. A. (1997). Upper crustal fluid migration: an example from the Variscides of SW Ireland. In *Journal of the Geological Society* (Vol. 154). https://www.lyellcollection.org

Meere, P. A., Mulchrone, K. F., & Timmerman, M. (2013). Shear folding in low-grade metasedimentary rocks: Reverse shear along cleavage at a high angle to the maximum compressive stress. *Geology*, *41*(8), 879–882. https://doi.org/10.1130/G34150.1

Mertoglu, O., Simsek, S., Basarir, N., & Paksoy, H. (2019). *Geothermal Energy Use, Country Update for Turkey*. European Geothermal Congress 2019 Den Haag.

Mitchell, W. I. (Ed.). (2004). *The Geology of Northern Ireland. Our Natural Foundation* (2nd ed.). Geological Survey of Northern Ireland. https://doi.org/10.1017/S0016756805380435

Möllhoff, M., & Bean, C. J. (2016). Seismic noise characterization in proximity to strong microseism sources in the Northeast Atlantic. *Bulletin of the Seismological Society of America*, *106*(2), 464–477. https://doi.org/10.1785/0120150204

Naylor, D. (1992). The post-Variscan history of Ireland. In J. Parnell (Ed.), *Basins on the Atlantic Seaboard: Petroleum Geology, Sedimentology and Basin Evolution* (62nd ed., Vol. 62, pp. 255–275). Geological Society. https://www.lyellcollection.org

O'Donnell, J. P., Daly, E., Tiberi, C., Bastow, I. D., O'Reilly, B. M., Readman, P. W., & Hauser, F. (2011). Lithosphere-asthenosphere interaction beneath Ireland from joint inversion of teleseismic P-wave delay times and GRACE gravity. *Geophysical Journal International*, *184*(3), 1379–1396. https://doi.org/10.1111/j.1365-246X.2011.04921.x

O'Reilly, B. M., Hauser, F., Ravaut, C., Shannon, P. M., & Readman, P. W. (2006). Crustal thinning, mantle exhumation and serpentinization in the Porcupine Basin, offshore Ireland: Evidence from wide-angle seismic data. *Journal of the Geological Society*, *163*(5), 775–787. https://doi.org/10.1144/0016-76492005-079

O'Reilly, B. M., Hauser, F., & Readman, P. W. (2010). The fine-scale structure of upper continental lithosphere from seismic waveform methods: Insights into Phanerozoic crustal formation processes. *Geophysical Journal International*, *180*(1), 101–124. https://doi.org/10.1111/j.1365-246X.2009.04420.x

O'Reilly, B. M., Hauser, F., & Readman, P. W. (2012). The fine-scale seismic structure of the upper lithosphere within accreted Caledonian lithosphere: Implications for the origins of the "Newer Granites." *Journal of the Geological Society*, *169*(5), 561–573. https://doi.org/10.1144/0016-76492011-128

O'Reilly, B. M., Kiyan, D., Fullea, J., Lebedev, S., Bean, C. J., Meere, P. A., & Chambers, E. L. (2021). DIG: A New Project to De-risk Ireland's Geothermal Energy Potential. *EGU General Assembly*.

Parkes, D., Busby, J., Kemp, S. J., Petitclerc, E., & Mounteney, I. (2020). The thermal properties of the mercia mudstone group. *Quarterly Journal of Engineering Geology and Hydrogeology*, *54*(2). https://doi.org/10.1144/qjegh2020-098

Pasquali, R., Allen, A., Burgess, J., Jones, G. L., & Williams, T. H. (2015). Geothermal Energy Utilisation-Ireland Country Update. *Proceedings World Geothermal Congress*, *April 2015*, 19–25. https://pangea.stanford.edu/ERE/db/WGC/papers/WGC/2015/01043.pdf

Pasquali, R., O'neill, N., Reay, D., & Waugh, T. (2010). The Geothermal Potential of Northern Ireland. In *Proceedings World Geothermal Congress*.

Piana Agostinetti, N., & Licciardi, A. (2015). SIM-CRUST Project - Seismic Imaging and Monitoring of the Upper Crust : Exploring the Potential Low-Enthalpy Geothermal Resources of Ireland. *World Geothermal Congress 2015*, *April*, 9.

Polat, G., Lebedev, S., Readman, P. W., O'Reilly, B. M., & Hauser, F. (2012). Anisotropic rayleigh-wave tomography of Ireland's crust: Implications for crustal accretion and evolution within the caledonian orogen. *Geophysical Research Letters*, *39*(4), 1–5. https://doi.org/10.1029/2012GL051014

Poulsen, S. E., Balling, N., Bording, T. S., Mathiesen, A., & Nielsen, S. B. (2017). Inverse geothermal modelling applied to Danish sedimentary basins. *Geophysical Journal International*, *211*(1), 188–206. https://doi.org/10.1093/gji/ggx361

Poulsen, S. E., Balling, N., & Nielsen, S. B. (2015). A parametric study of the thermal recharge of low enthalpy geothermal reservoirs. *Geothermics*, *53*, 464–478. https://doi.org/10.1016/j.geothermics.2014.08.003

Quinn, M. F. (2006). *Lough Neagh: the site of a Cenozoic pull-apart basin*.

Raine, R., & Reay, D. (2019). *A review of geothermal reservoir properties of Triassic, Permian and Carboniferous sandstones in Northern Ireland*. www.bgs.ac.uk/gsni/

Reay, D. M. (2004). Geophysics and Concealed Geology. In W. I. Mitchell (Ed.), *The Geology of Northern Ireland, Our Natural Foundation* (pp. 227–248). The Geological Survey of Northern Ireland.

Reinecker, J., Gutmanis, J., Foxford, A., Cotton, L., Dalby, C., & Law, R. (2021). Geothermal exploration and reservoir modelling of the united downs deep geothermal project, Cornwall (UK). *Geothermics*, *97*. https://doi.org/10.1016/j.geothermics.2021.102226

Scheck-Wenderoth, M., Cacace, M., Maystrenko, Y. P., Cherubini, Y., Noack, V., Kaiser, B. O., Sippel, J., & Björn, L. (2014). Models of heat transport in the Central European Basin System: Effective mechanisms at different scales. *Marine and Petroleum Geology*, *55*, 315–331. https://doi.org/10.1016/j.marpetgeo.2014.03.009

Scheck-Wenderoth, M., & Maystrenko, Y. P. (2013). Deep control on shallow heat in sedimentary basins. *Energy Procedia*, *40*, 266–275. https://doi.org/10.1016/j.egypro.2013.08.031

Serpen, U., & DiPippo, R. (2022). Turkey - A geothermal success story: A retrospective and prospective assessment. *Geothermics*, *101*. https://doi.org/10.1016/j.geothermics.2022.102370

ShallowTHERM. (2021). *ShallowTHERM*. ShallowTHERM Webpage. http://irishgroundtherm.com/results-2/

Shannon, P. M. (2018). Old challenges, new developments and new plays in Irish offshore exploration. *Petroleum Geology Conference Proceedings*, *8*(1), 171–185. https://doi.org/10.1144/PGC8.12

Somerton, W. H. (1992). Chapter V. Thermal Conductivity of Rock/Fluid Systems. In W. H. Somerton (Ed.), *Thermal properties and temperature-related behavior of rock/fluid systems* (Vol. 37, pp. 39–81). Elsevier. https://doi.org/https://doi.org/10.1016/S0376-7361(09)70025-1

Torne, M., Jiménez-Munt, I., Negredo, A. M., Fullea, J., Vergés, J., Marzán, I., Alcalde, J., Gómez-Rivas, E., & de la Noceda, C. G. (2023). Advances in the modeling of the Iberian thermal lithosphere and perspectives on deep geothermal studies. *Geothermal Energy*, *11*(1), 3. https://doi.org/10.1186/s40517-023-00246-6

van den Berg, R., Daly, J. S., & Salisbury, M. H. (2005). Seismic velocities of granulite-facies xenoliths from Central Ireland: Implications for lower crustal composition and anisotropy. *Tectonophysics*, *407*(1–2), 81–99. https://doi.org/10.1016/j.tecto.2005.07.003

Vilà, M., Fernández, M., & Jiménez-Munt, I. (2010). Radiogenic heat production variability of some common lithological groups and its significance to lithospheric thermal modeling. *Tectonophysics*, *490*(3–4), 152–164. https://doi.org/10.1016/j.tecto.2010.05.003

Vozar, J., Jones, A. G., Campanya, J., Yeomans, C., Muller, M. R., & Pasquali, R. (2020). A geothermal aquifer in the dilation zones on the southern margin of the Dublin Basin. *Geophysical Journal International*, *220*(3), 1717–1734. https://doi.org/10.1093/gji/ggz530

Wawerzinek, B., Ritter, J. R. R., Jordan, M., & Landès, M. (2008). An upper-mantle upwelling underneath Ireland revealed from non-linear tomography. *Geophysical Journal International*, *175*(1), 253–268. https://doi.org/10.1111/j.1365-246X.2008.03908.x

Wheildon, J., Gebski, J. S., & Thomas-Betts, A. (1985). *Further Investigations of the UK Heat Flow Field (1981-1984)*.

Willmot Noller, N. M., & Daly, J. S. (2015). The Contribution of Radiogenic Heat Production Studies to Hot Dry Rock Geothermal Resource Exploration in Ireland. *World Geothermal Congress 2015*, *April*, 19–25.

Woodcock, N., & Strachan, R. A. (2009). *Geological History of Britain and Ireland*. John Wiley and Sons.

Yeomans, C. M. (2011). *Geothermal implications of the Mourne Mountains: constraints from magnetotelluric modelling* [Masters Thesis]. University of Birmingham.

Younger, P. L., Gluyas, J. G., & Edryd Stephens, W. (2012). Development of deep geothermal energy resources in the UK. *Energy*, *165*(EN1), 19–32. https://doi.org/10.1680//ener

9 Figures

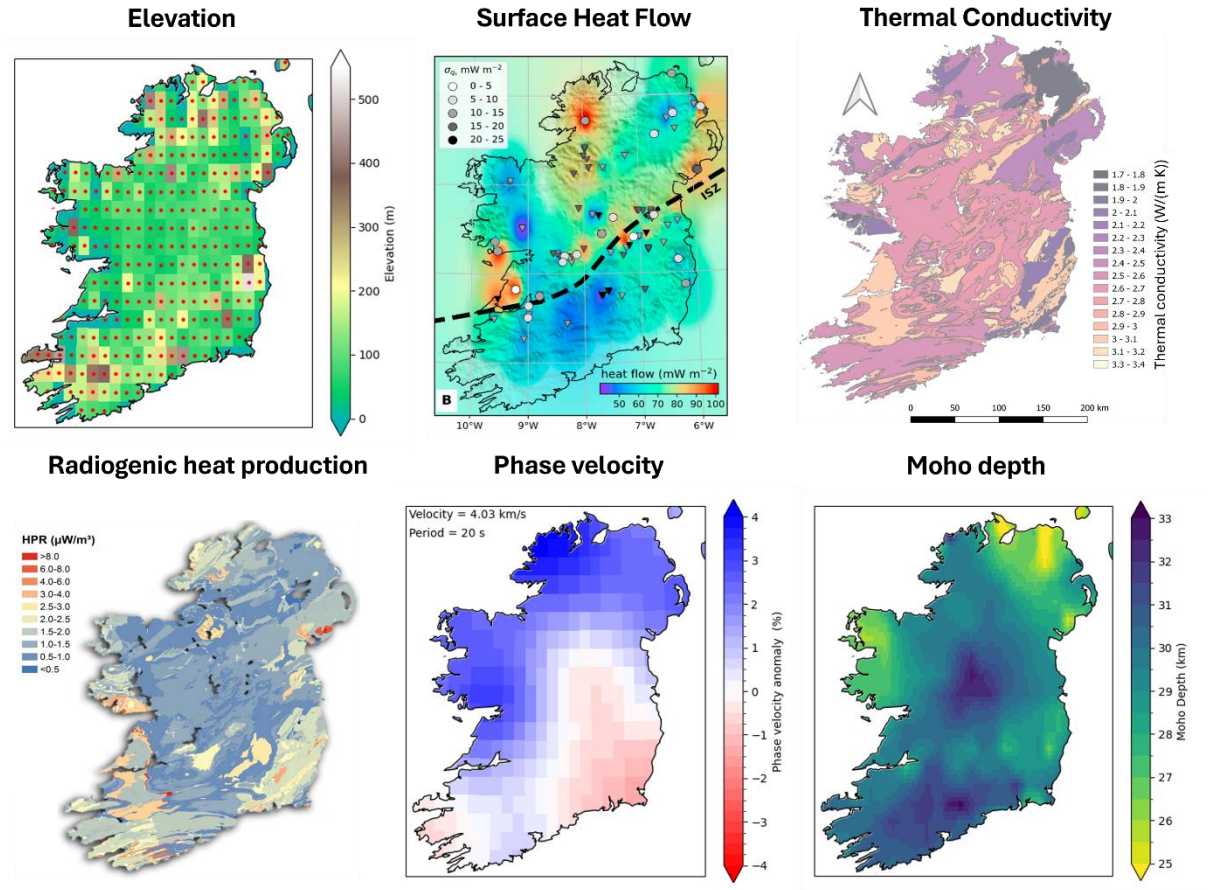

Figure 1 Input datasets used in the joint geophysical-petrological inversion. These include Elevation from ETOPO1 (Amante & Eakins, 2009), surface heat flow (Mather et al., 2018), thermal conductivity (Chambers et al., 2023), radiogenic heat production (Willmot Noller & Daly, 2015), Love- and Rayleigh-wave phase velocities (Bonadio et al., 2021; Chambers et al., 2023) with Love-waves at 20 s shown here. Reference phase velocity is in the upper left corner. and Moho depth which is a combination of the models of Bonadio et al., (2021) and Licciardi et al., (2014, 2020). The red points on the elevation show the points used in the inversion with a grid spacing of 0.2° x 0.2° which is the same of the Love-wave phase velocity resolution.

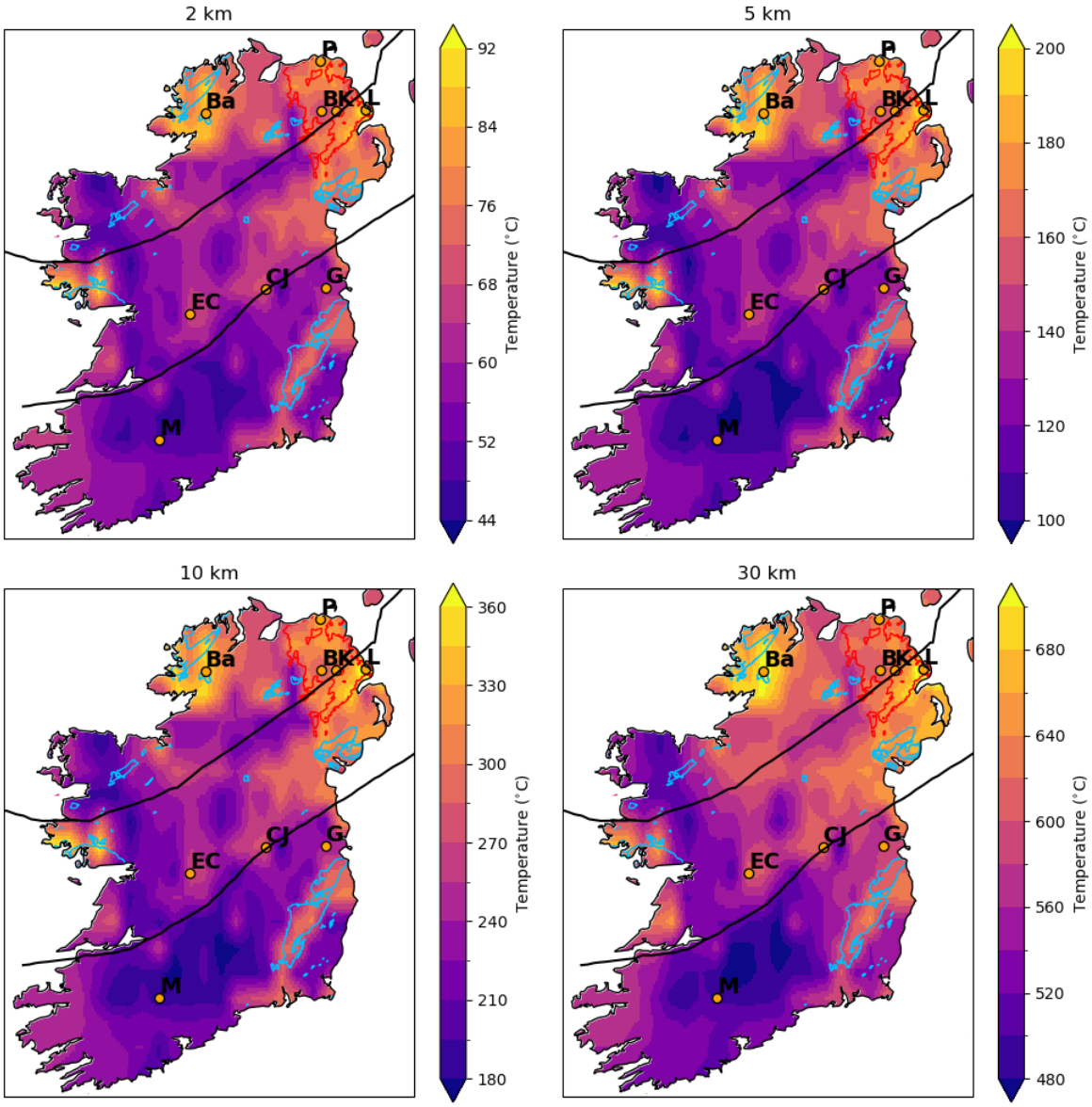

Figure 2 Subsurface temperature maps of the island of Ireland at 2, 5, 10 and 30 km depth. Data has been cropped to the coastline and smoothed. The Iapetus Suture Zone marked by thick black lines, Basaltic bedrock as red polygons and granites by light blue line (Bedrock units taken from the GSI bedrock geology viewer (Geological Survey Ireland, 2020)*). Orange points are locations referred to in the text and 1D columns shown in Figure 8. Acronyms are: B – Ballymacilroy, Ba – Barnesmore Donegal, CJ – Castle Jordan, EC – Eyres Court, G – Grangegorman, K – Kells (NI), L – Larne, M – Mallow, P – Portmore.*

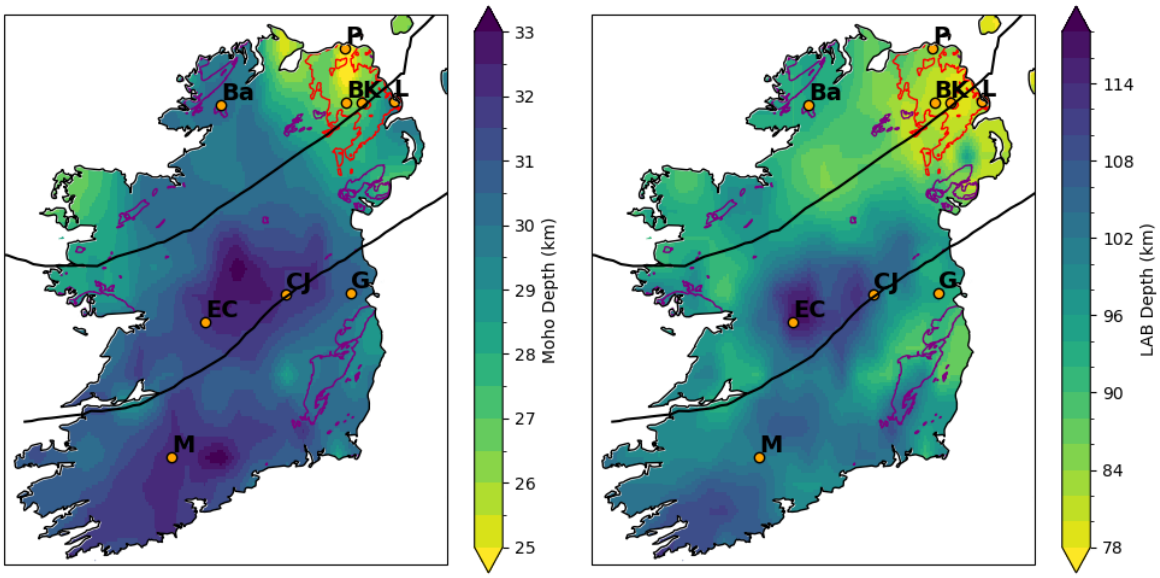

Figure 3 a) Moho and b) Lithosphere Asthenosphere Boundary (LAB) maps of Ireland. The thickest crust and lithosphere is in central and southern Ireland whereas thinner crust and a shallower LAB are beneath Northern Ireland, the north of the island and at Mayo and Galway on the west coast. See Figure 2 for symbol descriptions.

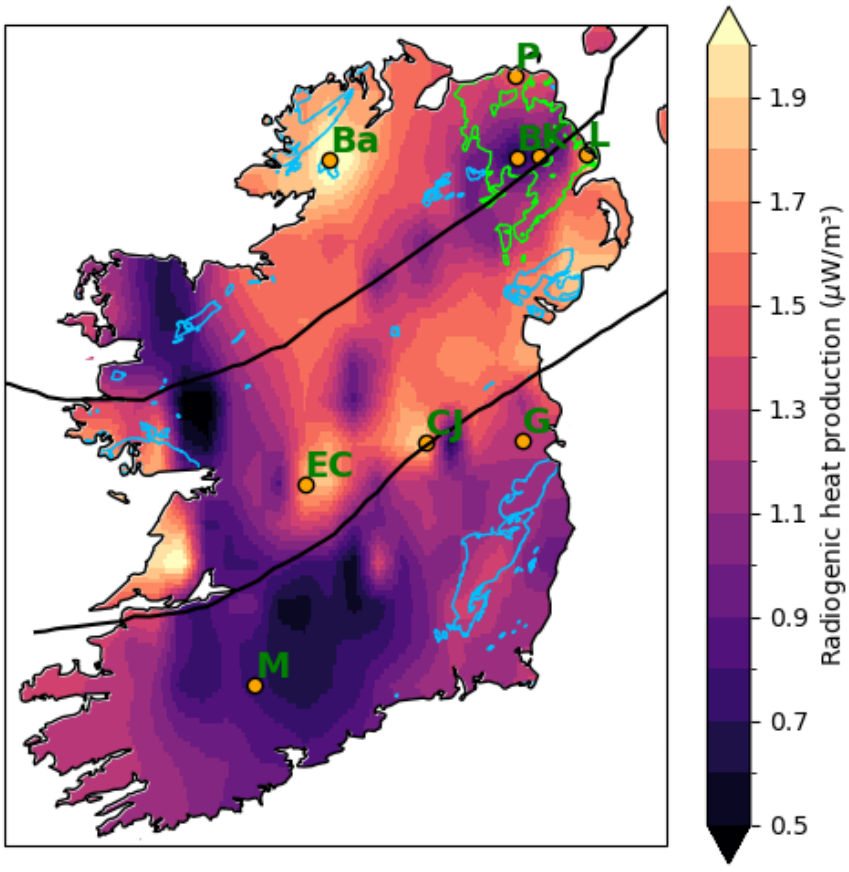

Figure 4 Radiogenic Heat Production (RHP) map from the inversion for Ireland. The highest RHP is beneath the granitic regions whereas the lowest are within the Iapetus Suture Zone and the south of Ireland. See Figure 2 for symbol descriptions.

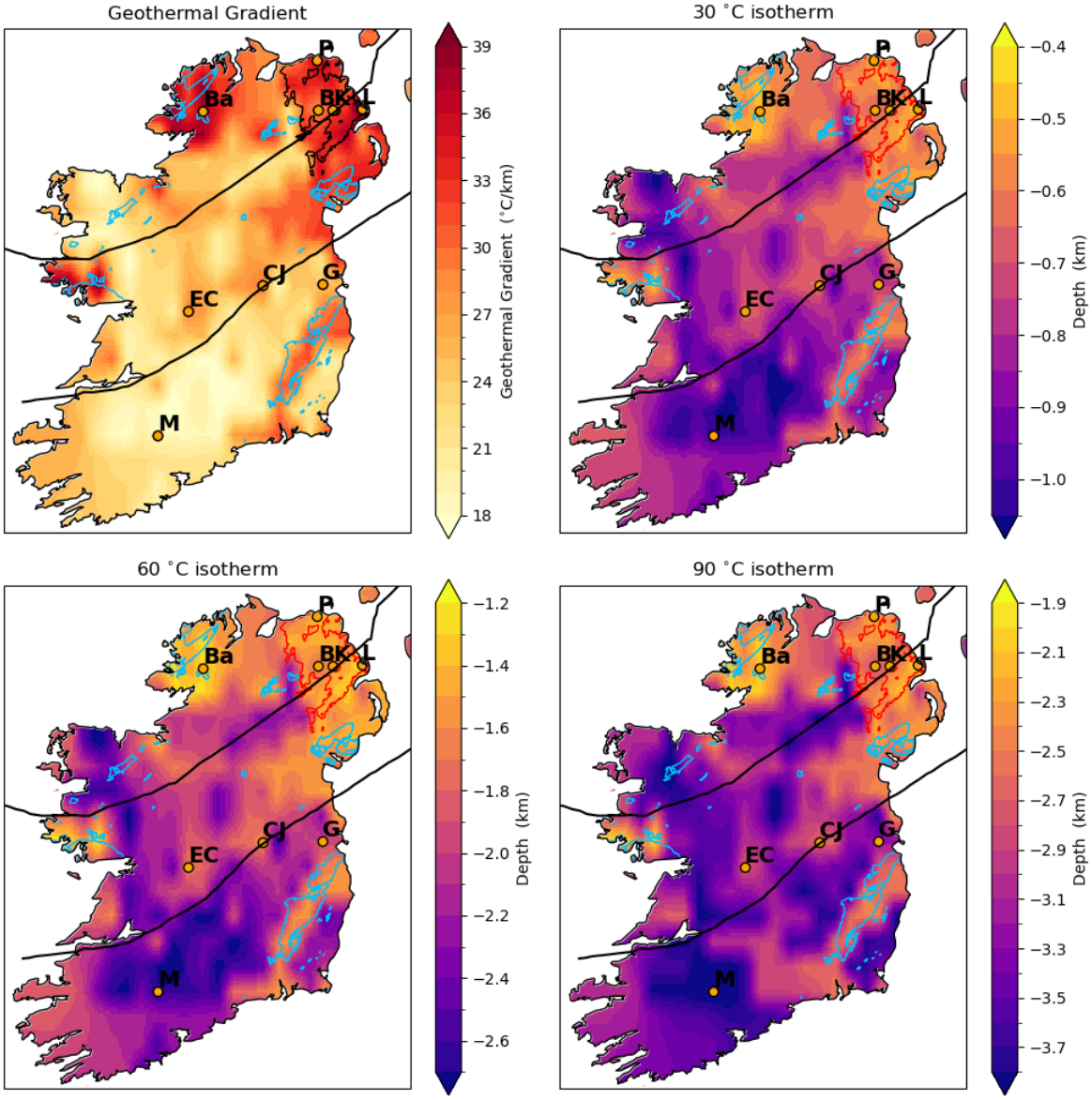

Figure 5 Geothermal Gradient map and depth to the 30, 60 and 90 °C isotherms. Note variable colour scales. See Figure 2 for symbol descriptions.

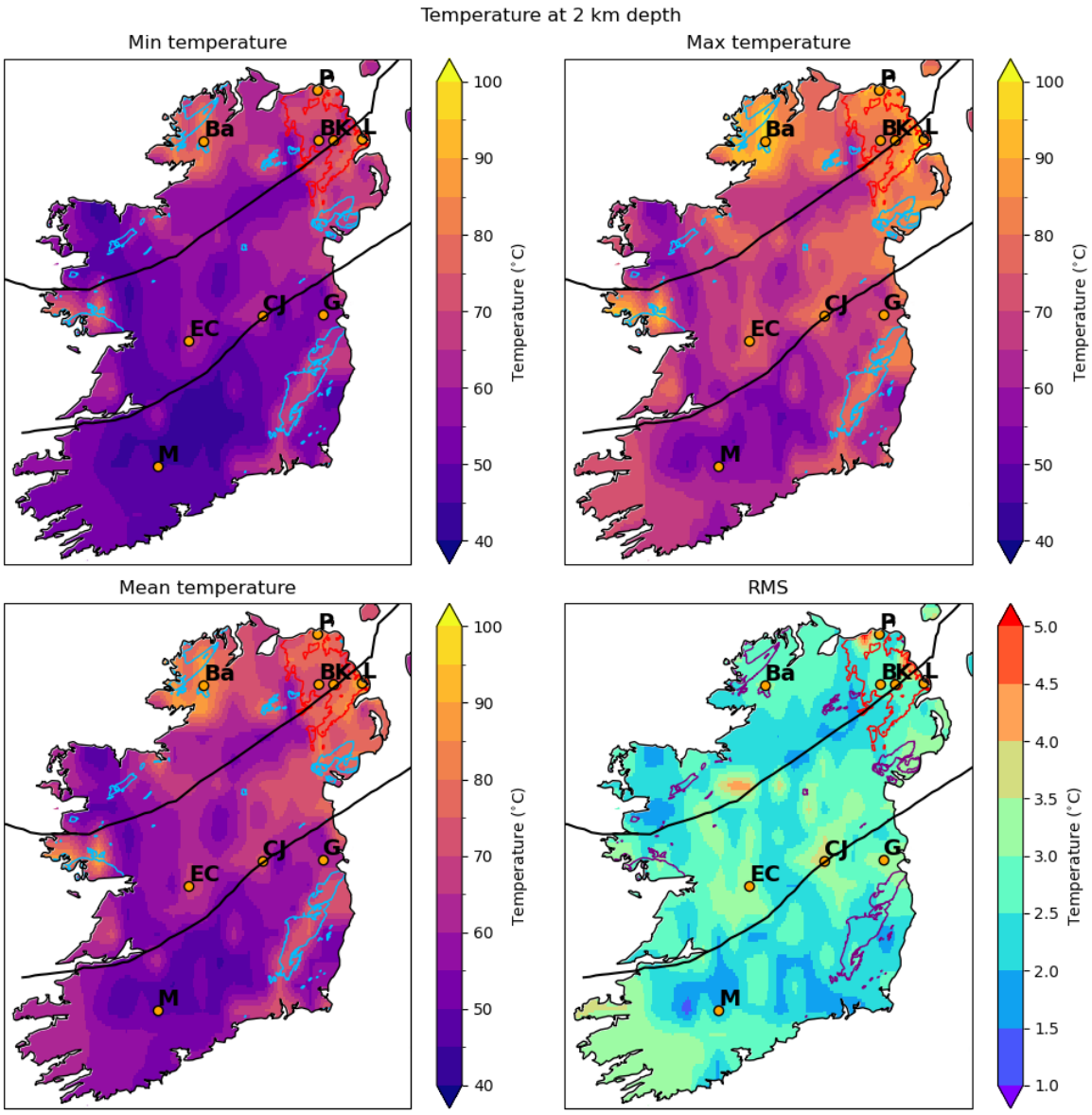

Figure 6 Uncertainty analysis for every point at 2 km depth. Minimum, maximum and the mean temperature for all possible input parameters are plotted. Uncertainty for the 2 km temperature slice is shown in the bottom right panel. See Figure 2 for symbol descriptions.

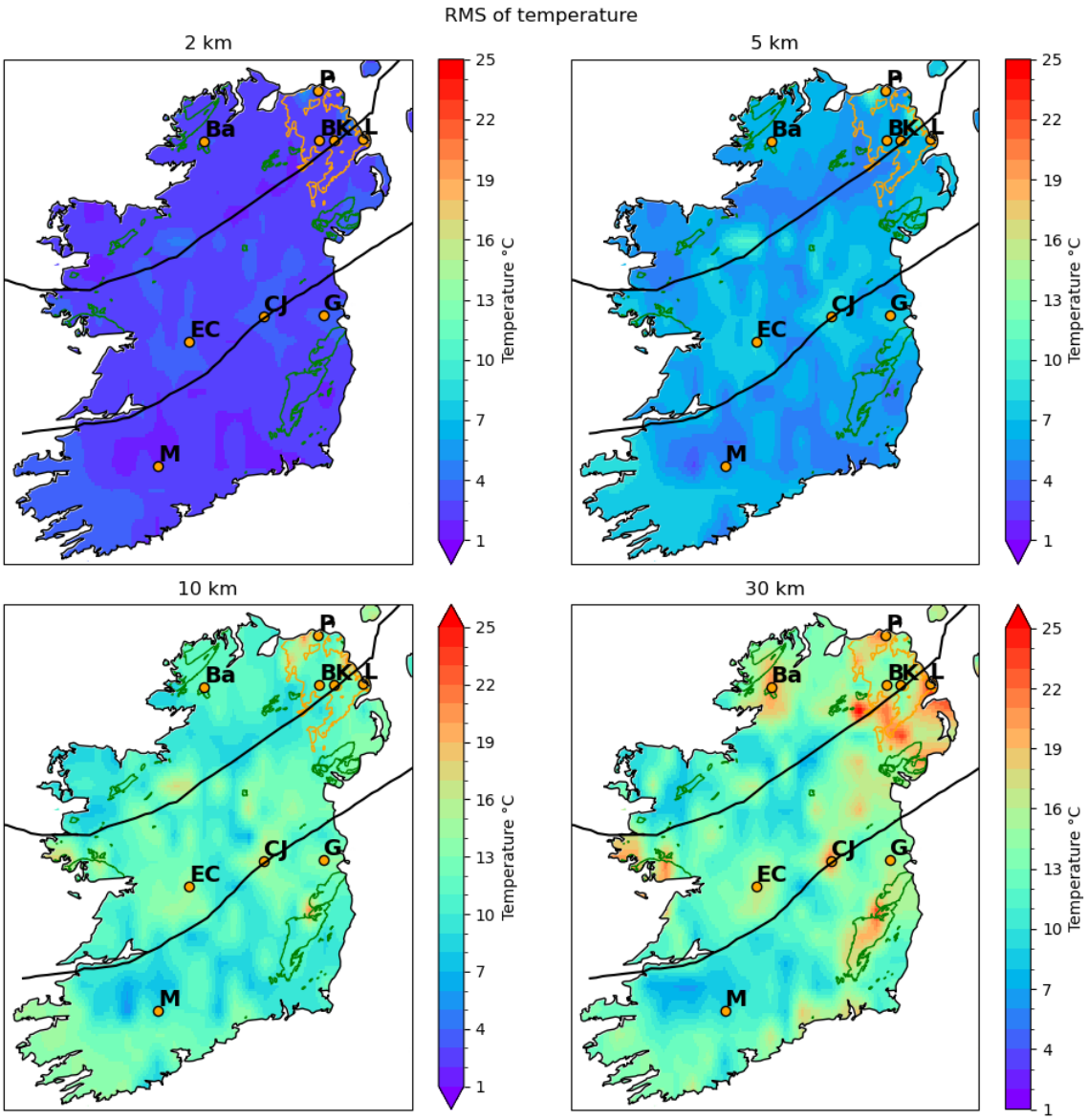

Figure 7 Uncertainty maps showing the temperature variation with increasing depth for our model. Depth slices at 2, 5, 10 and 30 km are shown. See Figure 2 for symbol descriptions.

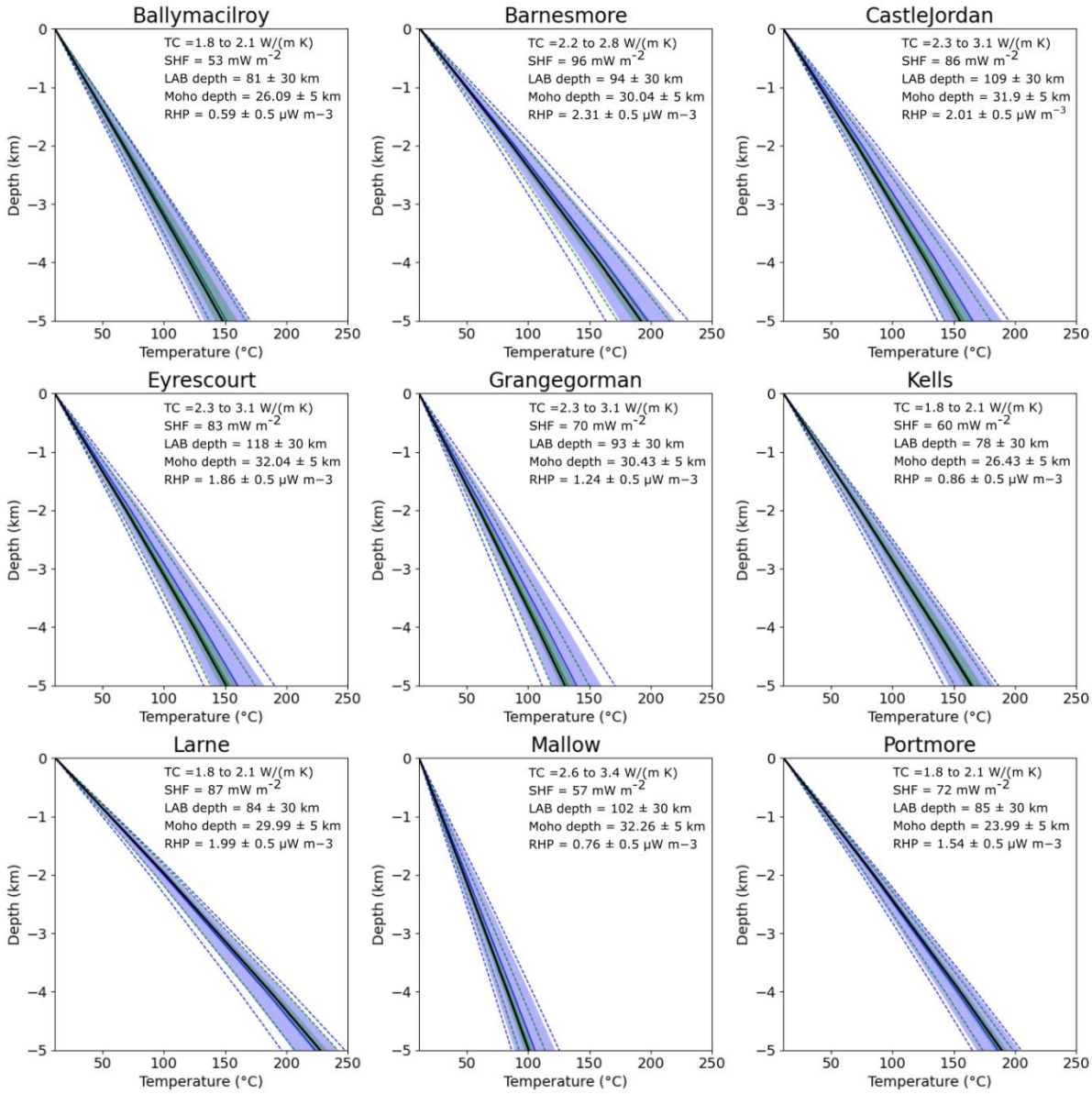

Figure 8 Uncertainty analysis for 9 columns with the best original input data from 0 to 5 km depth. The best temperature is plotted as a thick black line and the green dashed lines show the minimum and maximum temperature for 1 fixed input parameter/variable at a time, with the mean indicated by the thick green line and the shaded region the standard deviation either side of the mean. The blue lines are the same as the green lines but for all the key input parameter/variable fixed within plausible ranges, see text for further details. The best temperature always plots within both standard deviations. The RMS and standard deviation are similar to one another so only standard deviation is shown here.

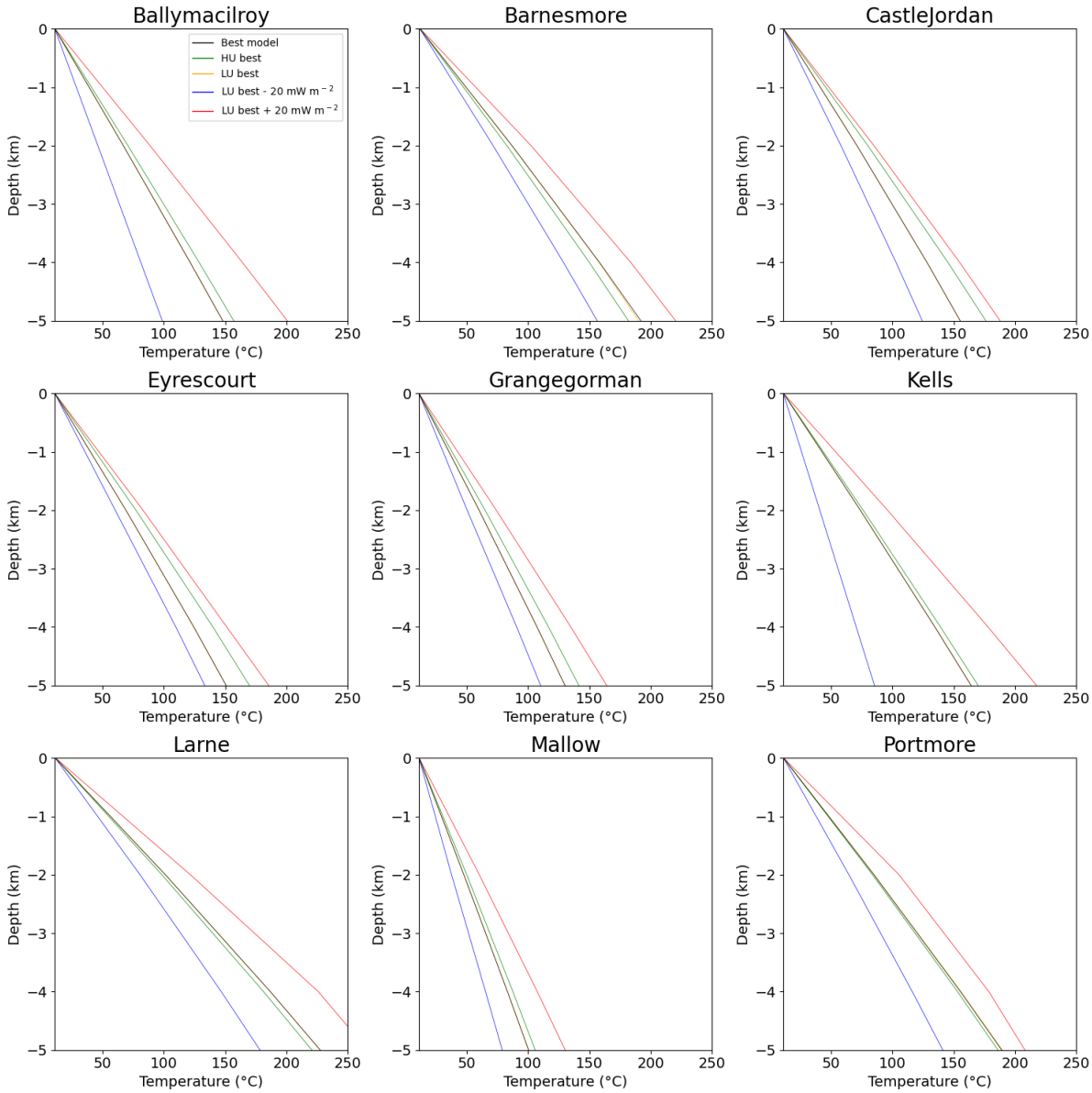

Figure 9 SHF sensitivity tests for each of the 9 columns. The original best model is shown by the black line and the green line is the best model with uncertainty in the SHF data increased to 20 mW m^{-2} (HU = High uncertainty). The Orange, blue and red lines are the second set of test for LU = Low Uncertainty, with orange the original SHF value, blue -20 mW m^{-2} from the original and red +20 mW m^{-2}. Uncertainty in the input data was reduced to 0.0001. As expected, the best and LU best models are very similar with the HU best model also close to the original best model.

Supplementary

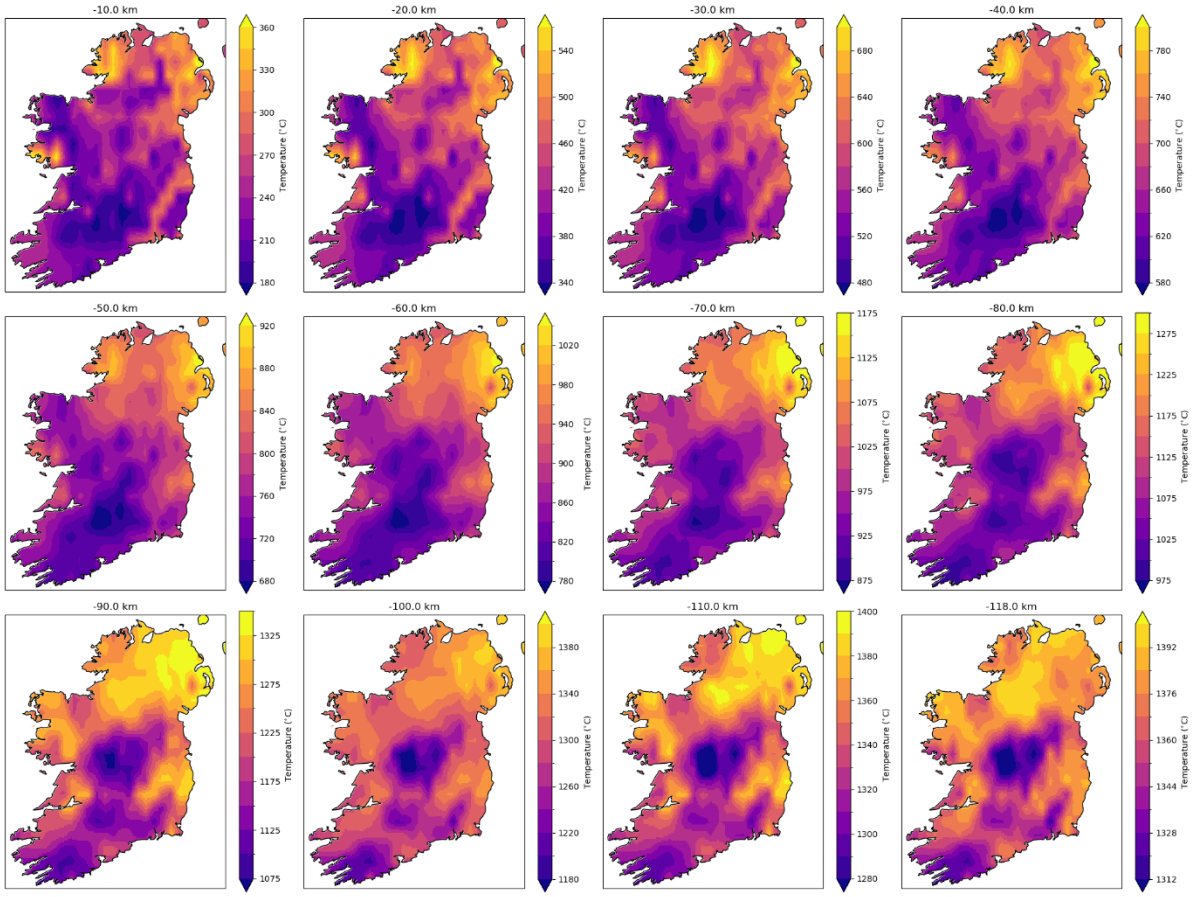

Supplementary Figure 1 Additional subsurface temperature maps from 10 km to 110 km depth in 10 km increments ending at 118 km.

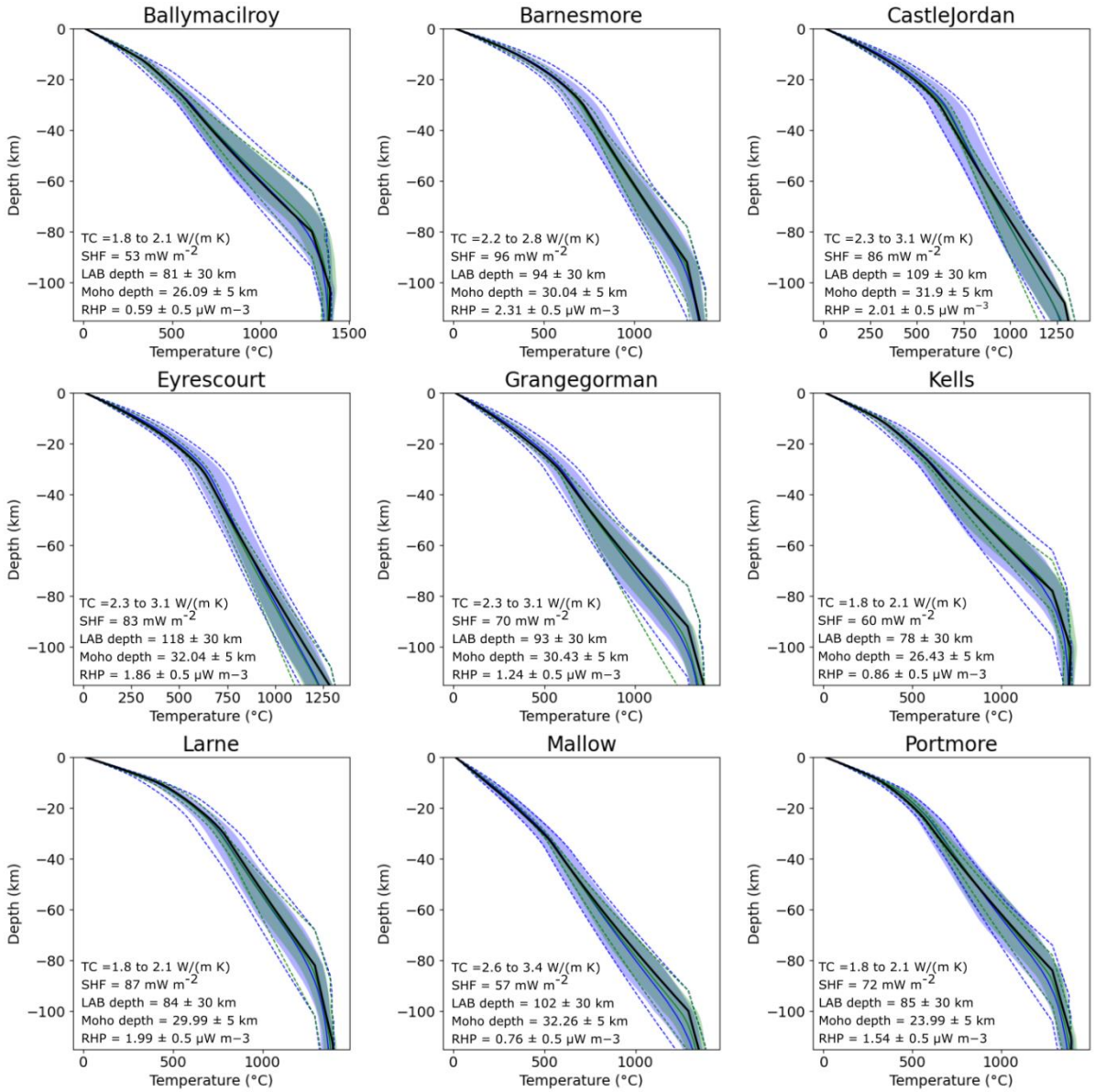

Supplementary Figure 2 Uncertainty analysis for 9 columns with the best original input data from 0 to 115 km depth. The best temperature is plotted as a thick black line and the green dashed lines show the minimum and maximum temperature varying 1 input parameter/variable at a time, with the mean indicated by the thick green line and the shaded region the standard deviation either side of the mean. The blue lines are the same as the green lines but for all the key input parameter/variable fixed within plausible ranges, see text for further details. The best temperature always plots within both standard deviations. The RMS and standard deviation are similar to one another so only standard deviation is shown here.

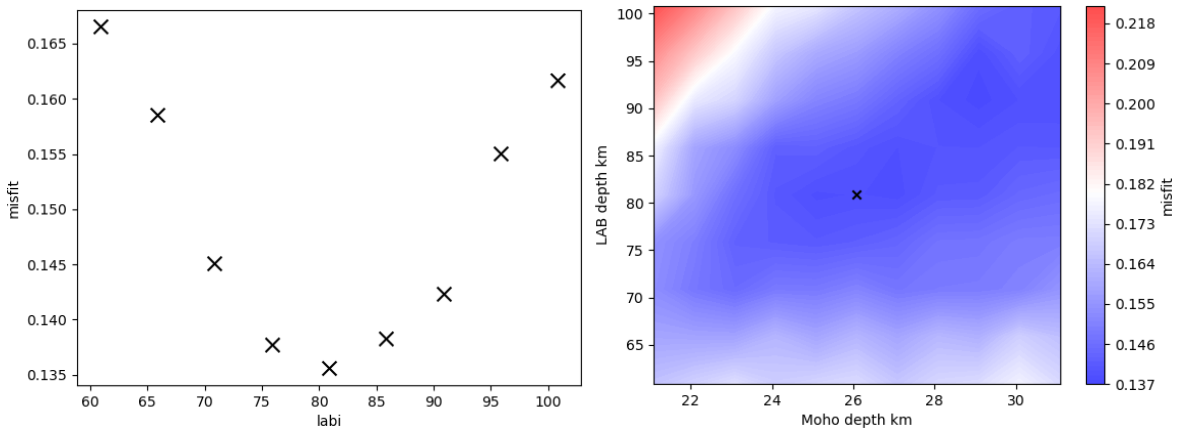

Supplementary Figure 3 Uncertainty analysis for column Ballymacilroy showing a) the variation in the misfit for changing LAB depth with fixed Moho depth and b) the contoured misfit for changes in Moho and LAB depth. Note the starting parameters are the output of the best temperature model.

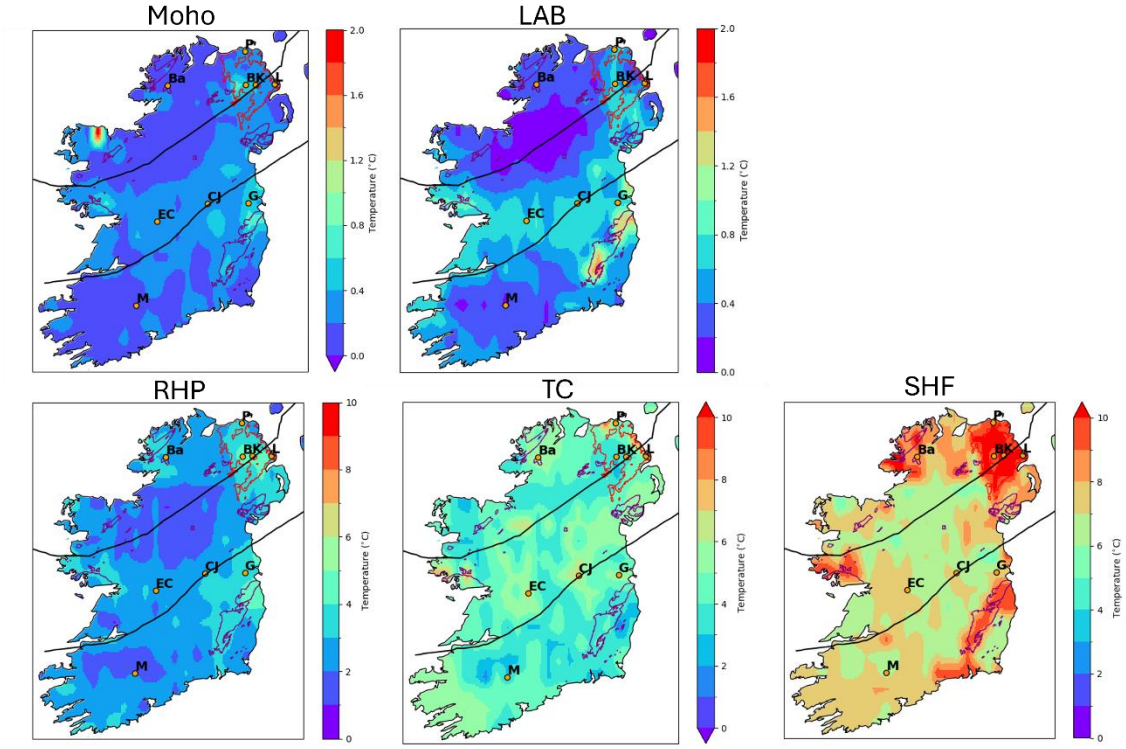

Supplementary Figure 4 Temperature uncertainty variation at 2 km depth associated with Moho, LAB (top row), RHP, TC and SHF (bottom row from left to right) uncertainties. Note variable colour scales for top and bottom plots. SHF is included to show the large variation when changing input data but overall the uncertainty is small and <±5 °C in most areas for individual input inversion parameters. See Figure 2 for symbol descriptions.

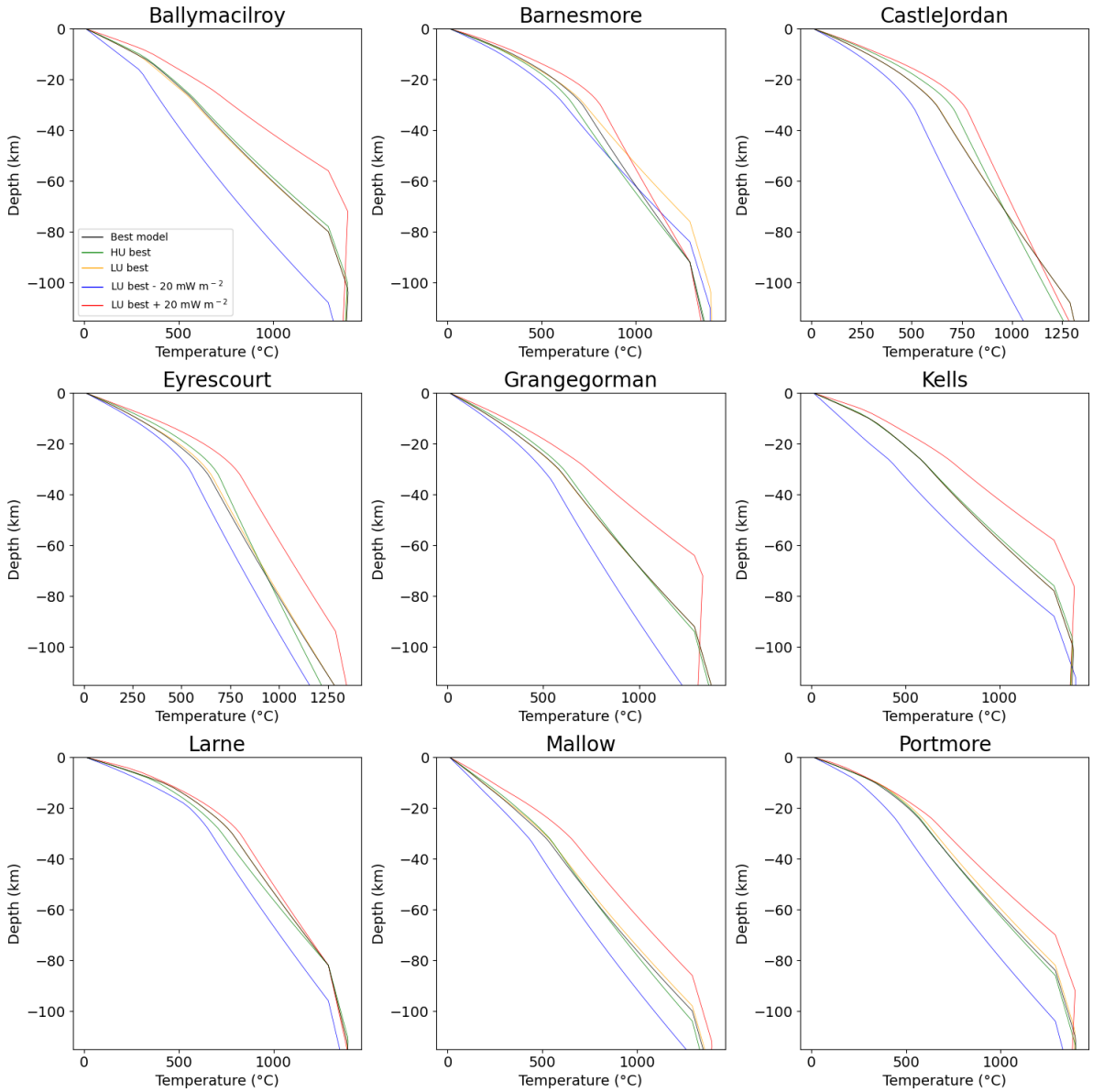

Supplementary Figure 5 Same as Figure 9. SHF sensitivity tests for each of the 9 columns for all depths. The original best model is shown by the black line and the green line is the best model with uncertainty in the SHF data increased to 20 mW m^{-2} (HU = High uncertainty). The Orange, blue and red lines are the second set of tests for LU = Low Uncertainty, with orange the original SHF value, blue -20 mW m^{-2} from the original and red +20 mW m^{-2}. Uncertainty in the input data was reduced to 0.0001. As expected, the best and LU best models are very similar with the HU best model also close to the original best model.